

FIRST PRINCIPLE COMPUTATIONAL
STUDIES ON HYDROGEN BOND SWITCH IN
BIOLOGICAL PROTON TRANSFER

By

SHUO DAI

Bachelor of Science in Physics

Nanjing University

Nanjing, China

2004

Submitted to the Faculty of the
Graduate College of the
Oklahoma State University
in partial fulfillment of
the requirements for
the Degree of
MASTER OF SCIENCE
July, 2013

FIRST PRINCIPLE COMPUTATIONAL
STUDIES ON HYDROGEN BOND SWITCH IN
BIOLOGICAL PROTON TRANSFER

Thesis Approved:

Dr. Aihua Xie

Thesis Adviser

Dr. John Mintmire

Dr. Donghua Zhou

ACKNOWLEDGEMENTS

First, I would like to thank my advisor Dr. Aihua Xie, who initiated and created this beautiful model, giving me a chance to perform research on this fascinating topic. During these years, she was very helpful and gave many wonderful suggestions to help me finish this project. Counting from the first mechanism, Grotthuss mechanism*, published in this field in 1806, it is 200 years. It is convinced that Dr.Xie will solve this problem, at least pushing it to the best level of current understanding. In addition to modeling work, she is also an excellent experimentalist who did great contributions in signaling and bioenergetics proteins field. Beside academic field, she also taught me many strategies to perform independent research as well as instructions on becoming professional, which is very important for a PhD student.

I would like to thank my advisory committee: Dr. Zhou and Dr. Mintmire for their encouragements and helpful supports. And although not in my master committee, but in my PhD committee: Dr. Rosenberger and Dr. Burnap gave many fantastic suggestions and helps. I really appreciate all your efforts. Especially, I want to thank Dr. Hoff for sharing me with many insights and offering me many helps in proton transfer project.

Also, I would like take this chance to appreciate the helps from all the faculty members and staff members. Their supports mean much to me. I want to thank the graduate students in the department and lab for the helpful and interesting discussions we once had, specially the lab members: Sandip, Zhouyang and Ningning.

Last, my great gratitude goes to my family. They supported me during all these years that I was abroad otherwise it is not possible for me to concentrate on research.

* De Grotthuss, C.J.T. (1806). "Sur la décomposition de l'eau et des corps qu'elle tient en dissolution à l'aide de l'électricité galvanique". *Ann. Chim.* **58**: 54–73.

Name: Shuo Dai

Date of Degree: JULY, 2013

Title of Study: FIRST PRINCIPLE COMPUTATIONAL STUDIES ON HYDROGEN
BOND SWITCH IN BIOLOGICAL PROTON TRANSFER

Major Field: PHYSICS

Abstract:

Proton transfer is fundamental to biological process. However, the factor that controls biological proton transfer in proteins is not clear yet. In our lab, we have developed a proton transfer model based on Photoactive Yellow Protein. Significant progresses have been made in understanding the molecular mechanism of proton transfer. In addition to the established structural elements, proton donor and proton acceptor, previous study on our model suggests a new structural element, which we named hydrogen bond switch. In this study, first principle computation is applied to explore the geometry of hydrogen bond switch, the control element for the direction of proton transfer. Our results show that geometry of hydrogen bond between proton donor and hydrogen bond switch, namely hydrogen bond length and hydrogen bond angle, affect the switch power for proton transfer. If H₂O is the hydrogen bond switch, then a net increment of 18.7kJ/mol in switch power can be acquired when switch-donor hydrogen bond length shortened from 3.00Å to 2.50Å. And results on hydrogen bond angle demonstrate that variations of hydrogen bond angle could only contribute a maximum of 10% in energy as much as hydrogen bond length does. We conclude that hydrogen bond with shorter length between the proton donor and hydrogen bond switch gives stronger switch power. In addition, changing the length of the hydrogen bond between proton donor and hydrogen bond switch has reversed the relative height of the two local minimums in the energy landscape. Finally, our calculations reveal that the switch power in dielectric environment could be reduced but the reducing effect that dielectric environment gave on hydrogen bond switch is less as dielectric constant becomes larger. This implies that taking dielectric environment into account, hydrogen bond switch still can provide enough switch power to proton transfer complex.

TABLE OF CONTENTS

I. INTRODUCTION	1
1.1 Proton Transfer in Proteins	1
1.2 Hydrogen Bonding Interaction in Proteins	3
1.3 Photoactive Yellow Protein	11
II. COMPUTATIONAL THEORIES AND METHOD	18
2.1 Atomic and Molecular Modeling (Quantum Mechanics Based)	18
2.2 Density Functional Theory	22
2.3 Method Used in This Study	26
III. IMPACT OF HYDROGEN BOND SWITCH ON PROTON TRANSFER	34
3.1 Geometry and Energy Landscape Analysis	34
3.2 Electronic Structure and Dielectric Environment	52
REFERENCES	56
APPENDIX A	61
APPENDIX B	65
APPENDIX C	73

LIST OF TABLES

Table 1-1 Techniques used to perform research on hydrogen bond.....	4
Table 1-2 Classification of hydrogen bonds	5
Table 1-3 Hydrogen bond donors in proteins	6
Table 1-4 Hydrogen bond acceptor in proteins.....	8
Table 2-1 Examples for different types of functionals	24
Table 3-1 Proton affinity for different DA distance (No switch).	35
Table 3-2 Proton affinity for different DA distance (H ₂ O as switch).....	35
Table 3-3 Proton affinity for different DA distance (Tyr as switch)	35
Table 3-4 Hydrogen bond energy in D state and the switch power.....	37
Table 3-5 Length of hydrogen bond between hydrogen bond switch and proton donor	38
Table 3-6 Energy barrier with different HB Bridge lengths without hydrogen bond switch	43
Table 3-7 Energy barriers with the different donor-acceptor and switch-donor distance.	43
Table 3-8 Energy barrier and Proton affinity in the different switch-donor or donor-acceptor distance	43
Table 3-9 Energy variation when donor-acceptor or switch-donor distance change	44
Table 3-10 Comparison of the change in bond length upon before and after proton transfer.....	50

LIST OF FIGURES

Figure 1.1 Active site structure of wild type PYP	12
Figure 1.2 The photocycle of PYP.....	12
Figure 1.3 Structural elements in proton transfer	14
Figure 1.4 The 3D potential energy surface.....	15
Figure 2.1 The illustration of a typical molecular group studied.....	29
Figure 2.2 Morse potential curves	31
Figure 2.3 Lennard-Jones potential curves	33
Figure 3.1 Switch power of different switch-donor hydrogen bond length..	37
Figure 3.2 The switch-donor hydrogen bond angle scan result.....	39
Figure 3.3 Histogram of the energy variation when angle changes from 100° to 140°	40
Figure 3.4 Comparison of molecular conformation at D and A state.....	41
Figure 3.5 Energy landscape of the system when H2O is hydrogen bond switch. (2.50Å-2.80Å).....	45
Figure 3.6 Energy landscape of the system when H2O is hydrogen bond switch. (2.80Å-3.00Å).....	46
Figure 3.7 Single Morse fitting to D state energy.....	47
Figure 3.8 Lennard-Jones potential fitting to the energy landscape of different switch-donor distances. (Tyr)	48
Figure 3.9 Lennard-Jones potential fitting to the energy landscape of different switch-donor distances. (H ₂ O).....	49
Figure 3.10 Structure of two hydrogen bond switch molecules.	50
Figure 3.11 Electron density map of three structural elements in proton transfer	53
Figure 3.12 Switch power of different proton transfer switch-donor distance in different dielectric environment.....	54

CHAPTER I

INTRODUCTION

1.1 Proton Transfer in Proteins

Proton transfer is one of the fundamental phenomena in biology and physics. Therefore, the understanding of its mechanism will enable us to better understand the structure and function of proteins and also provide us with the connection to the mechanism of other molecular process in the field of biology (e.g. protein quake[1]) In addition, from the physics point of view, proton transfer is one kind of quantum transport phenomena. So the mechanism study of proton transfer in protein will also make up a fundamental knowledge in the field of physics.

In most kinds of proteins, proton transfer plays a role in their structure and function. In the category of bioenergetics proteins, for example, Bacteriorhodopsin performs its function by utilizing the proton transfer to build up the electro-chemical potential across the membrane. In the category of signaling protein, for example, Photo active Yellow Protein (PYP)[2, 3] uses proton transfer to create conformational change so as to bind to its downstream partner. More

examples show that It is important to study proton transfer so as to enlarge our understanding in the structure-function paradigm in proteins.

The proton transfer in proteins: structures

From the studies in the last 200 years in the field, people concluded two structural elements [4] in proton transfer: proton donor and proton acceptor. Proton donor is the molecule that donates the proton to the proton acceptor. The most common donors and acceptors are from the side chains of amino acids. However, sometimes other molecules could also act as the donor or acceptor. The Chromophore of PYP is an example that non-amino acid acts as proton acceptor.

The complicate property of proton donor and acceptor in protein poses challenges to the researchers. In aqueous solution, it is generally correct that proton moves from group that has lower pKa to the group that has higher pKa. But this rule is different in proteins. First, the pKa value of certain function group in proteins is not necessarily the same as the one in aqueous solutions. Its value is depends on its position in the proteins. For example, Glu 46 in PYP has a pKa value of 10 [2], which is much higher than its value in aqueous solution. This makes it difficult to find out value of pKa. Second, even for the same group, the pKa value is dynamically changed while the protein performing its function. For example, Asp96 in Bacteriorhodopsin[5] has pKa higher than 12 in bR state and has pKa nearly 6.7 in N state. All these difficulties prevent pKa method from becoming a popular method in determining the proton transfer direction.

The proton transfer in protein: Function

Proton transfer is a kind of charge transfer. If there is ionization, a net charge will appear. Then through process of proton transfer, the charge could be delivered through hydrogen bond. For example, in PYP which is a signaling protein, the proton transfer brings the charge from Glu46 to

chromophore, which result in instability of charge distribution and protein quake will then be triggered[6].

Proton transfer is a kind of energy transfer. For example, Bacteriorhodopsin uses proton transfer to build up the electro-chemical potential[7]. The energy in the potential is the energy source for ATP molecule, which could directly help to start many important biochemical reactions.

Besides these functions, proton transfers also present in specific occasions, where only proton transfer could be used. Examples include many enzymes that use acid-base catalysis principle as their enzymatic cycle. These highly specific, highly efficient catalysts cannot work without proton transfer.

A partial list of proteins that use proton transfer as their function is attached as appendix C. Here just mention a few famous examples. Singling proteins include *Photoactive Yellow Protein (PYP)* and *Rhodopsin* proton transfer related proteins. Bio-energetics proteins include *Bacteriorhodopsin (bR)*, *Photosystem II* and *ATPase* used proton transfer to achieve part of their function. Enzymes include *Human Carbonic Anhydrase II (HCAII)* and *Ni-Fe hydrogenase* utilize proton transfer as the mechanism of the biochemical reaction that they catalyzed.

1.2 Hydrogen Bonding Interactions in Proteins

In most cases, the proton transfer is connected with hydrogen bond (HB). So the field of hydrogen bond research provides foundation to the research of proton transfer.

Definition of Hydrogen Bonds

The current definition of hydrogen bonds could be described from two points of view. The one below is the experiment of view. This is from the book [8]: "The hydrogen bonds are formed between donor group D-H and acceptor group A, when the electro-negativity of D in D-H group is

such as to withdraw electrons and leave the proton partially unshielded and the acceptor A must have lone-pair electrons or polarizable π electrons in order to interact with donor group.”

Also the hydrogen bond definition from international union of pure and applied chemistry (IUPAC)’s recommendation: “The hydrogen bond is an attractive interaction between a hydrogen atom from a molecule or a molecular fragment X-H in which X is more electronegative than H, and an atom or a group of atoms in the same or a different molecule, in which there is evidence of bond formation.”

Another point of view is from theoretical or result of computation, which can be found in the book[9].

Properties of Hydrogen Bond and classification

People have used many experimental techniques to investigate the hydrogen bond and different techniques could reveal different properties of HB. (Refer to Table1.1)

There are many ways to classify the hydrogen bonds. Based on the bond length or bond energy of hydrogen bond, we can then classify hydrogen bond into many categories. The one suggested by Emsley[10] divides the hydrogen bonds into two categories and later researchers expanded this classification to three categories. This is shown in Table 1.2.

Table1. 1 Techniques used to perform research on Hydrogen Bond.

Experimental Techniques	Properties to detect
IR, Raman, rotational spectroscopy	bond motions and local structure
NMR	electronic environment, re-orientation of bond vector
X-ray, Neutron Diffraction	bond length and other geometry parameters
X-ray Absorption Spectrum	Local chemical environment
Thermodynamics	bond energy
Transient vibrational holeburning and three pulse echoes	rearrangements of the HB network
Quantum chemistry calculation	bond energy and conformation around the energy minima

Table 1.2 Classification of hydrogen bonds.

D-H...A, where ... represents HB.	Strong	Moderate	Weak
Distance of A to B (Å)	2.2-2.5	2.5-3.2	3.2-4.0
Angle of D-H...A	175-180°	130-180°	90-180°
Lengthening of D-H (Å)	0.05-0.2Å	0.01-0.05Å	<0.01Å
Bond energy (kJ/mol)	63-167	17-63	<17
Example	Acid salts, HF complexes	Phenols, all Biological molecule	C-H , or π as donor
	P-OH...O=P	O-H...O=C	

Among all the techniques, Infrared spectroscopy methods provide a sensitive way to detect hydrogen bond[11]. In general, the D-H stretching mode will show changes in frequency, bandwidth and intensity. Recently, both blue shifted and red shifted hydrogen bond has been found[12]. It is also now understand, both the two are formed because the optimal bond length changed when the D-H group is hydrogen bonded. Depending on whether the new equilibrium length is longer or shorter than the original band length, the IR signals could show red shift or blue shift.

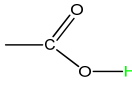
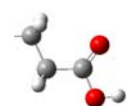
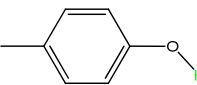
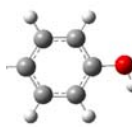
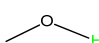

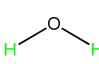
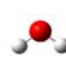
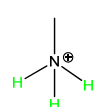
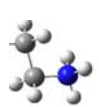
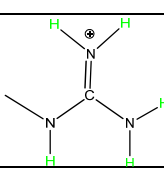

From the research methods available today, researchers could acquire the information of hydrogen bond from geometry (mechanical and electronic), energy and thermodynamic aspects. These are also the aspects of the discussion to be covered in later chapters.

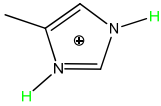

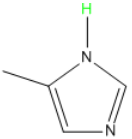
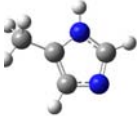
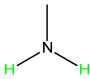
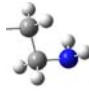
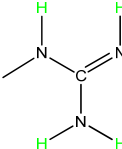
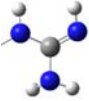
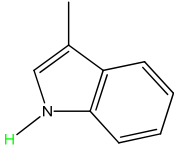

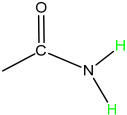
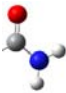
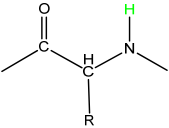
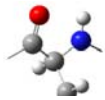
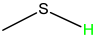

Hydrogen Bond Donors and Acceptors

It may be useful to provide a hydrogen bond donor and acceptor candidates in proteins. The partial list is shown in Table 1.3 and 1.4 .

The donor table is arranged according to the –OH, -NH, SH order and from charged group to neutral ground order. Because the hydrogen bond switch is essentially the hydrogen bond donor, what we chose to investigate are some representative molecules from each of the category, so as to make them comparable to each other.

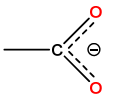
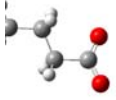
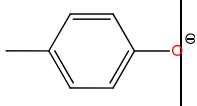

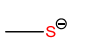

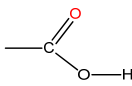

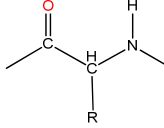

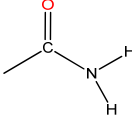

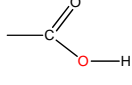
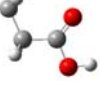
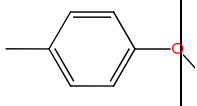

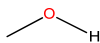

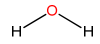
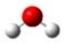
Table1- 3 Hydrogen bond donors in proteins

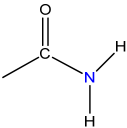
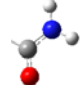
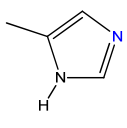

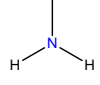
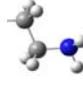
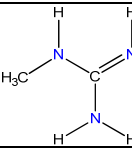

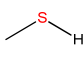

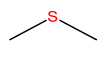

	Residue Name	Chemical structure	3D structure	Comments
OH	Asp[0] Glu [0]			
	Tyr[0]			
	Ser/Thr			
	H ₂ O			
NH	Lys[+]/N-terminus			
	Arg[+]			

	His[+]			
	His[0]			
	Lys[0]			
	Arg[0]			
	Trp			
	Asn/Gln			
	Backbone			
SH	Cys[0]			Could form disulfide bond

Because we are going to build up the proton transfer model, which involves the hydrogen bond interaction, we need to know the current study in HB modeling so as to correctly choose computation method.

Table1. 4 Hydrogen bond acceptor in proteins

	Residue Name	Chemical Structure	3D structure	Maximum Number of Hydrogen Bond	Comments
R ⁻	Asp[-] Glu[-] C-terminus			O,S: 3	Asp is shown more in bioenergetics and catalysis.
	Tyr[-]				
	Cys[-]				
C=O	Asp[0] Glu [0]			O: 3	Glu is shown more in signaling.
	Backbone				
	Asn/Gln				
-OH	Asp[0] Glu [0]			O: 2	
	Tyr[0]				
	Ser/Thr				
	H2O				

N	Asn/Gln			N:1	
	His [0]				
	Lys[0]				
	Arg[0]				Arg[0] is rarely seen in proteins. The maximum number of HBs is 3.
-S-	Cys[0]			S: 2	
	Met				

Later, in Coulson's paper, he used 5 orthogonal wave functions to investigate the O...O Hydrogen bond with bond length of 2.80Å. And the conclusion is the electrostatic force is about 65%. And the wave function he used as well as the methodology also becomes what is called "Coulson-Fischer" wave function and still used today to study molecular disassociation problem.

After molecular orbital theory (MO) was developed, researchers also tried to decomposing the energy in terms of molecular orbital theory. What is known as Morokuma decomposition method[13] is one way for doing this. According to this method, the total energy was decomposed into 5 kinds of interactions.

Electrostatic interaction is described by coulomb law, which including monopole-monopole, monopole-dipole, dipole-dipole and higher terms. Polarization is the distortion of e⁻ cloud by heavy atoms. Exchange repulsion is short-range repulsion of the electron distribution of

the donor and acceptor. Charge-transfer refers to electron transferred to empty orbital from donor (accepter) to acceptor (donor). Coupling is the coupled part of the above four kinds of energy.

Using this method, analysis showed[14] that the polarization and dispersion components form 48% of total energy of the hydrogen bond in a water dimer when the distance of two Oxygen atom is 2.98Å. If the distance becomes shorter, e.g. 2.5Å, then these interactions will account for 85% of the total energy. If the distance becomes longer, e.g. 3.2Å, then these interactions will account for 33% of the total energy.

To correctly model the hydrogen bond, we must take polarization and dispersion into account. This will help us to choose both correct and efficient method and basis set that has better cost/accuracy ratio. (DFT with 6-311+G(2d,p) basis set).

Hydrogen bond in proteins

Back to the 1950s, researchers have realized the importance of hydrogen bond for proteins to maintain the secondary structures (e.g. α -helix and γ -helix by Pauling and coworkers[15], parallel and anti-parallel β -sheet by Pauling and coworkers[16]). From the table 1.3 and table 1.4, we could find the backbone structure could be both HB acceptor and HB donor. Because of this, the hydrogen bond networks through backbone are able to have cooperative property [17, 18].

Hydrogen bond (HB) is important for it has its place in helping protein maintain its structure and thus carry out its function. For example, in common α -helix structure, the N-H group at n th position will form hydrogen bond with C=O group at $n-4$ th, which is essential to maintain this 2nd structure[19]. Aside from maintaining the secondary structure, hydrogen bonds found in active site also help in carrying out major function of protein. For example, in Photoactive Yellow Protein (PYP, a signaling protein), G46A mutant has the rate constant for its photocycle ~100 times larger than wildtype[20]. And the difference between them is the hydrogen bond between 46th residue and Chromophore in the active site does not exist in G46A, while wildtype has this

hydrogen bond. In Bacteriorhodopsin (a bio-energetic protein), the E85A mutant and E85Q (hydrogen bonding network changed from wildtype) are ~100 folds slower in forming the next intermediates state [21, 22].

In addition to providing the mechanical interconnection to the protein, Hydrogen bonds also play an important role in building protein's electronic structure. For example, replacement or removal of the hydrogen bond in the active site of PYP will cause spectral shift. In the wildtype PYP, the maximum of its absorption is at 446nm for pG state. And in E46Q mutant, where the 46th residue (Glutamate in wildtype) is replaced by Q (Glutamine), the strength of the hydrogen bond between 46th residue and chromophore is changed. Therefore, the maximum of its absorption is red-shifted to 462nm[23]. Then in E46A mutant, where the hydrogen bond is removed, the maximum of its absorption is red-shifted to 469nm[24]. Another example is Y42F mutant, where hydrogen bond between 42th residue and chromophore is removed. The maximum of its absorption is also red-shifted to 458nm[25].

1.3 Photoactive Yellow Protein (PYP)

PYP was first discovered from a halophilic purple photosynthetic bacterium, *Ectothiorhodospira Halophila*[26] which was later renamed to *Halorhodospira Halophila*. This protein consists of 125 amino acids and the function of this protein is blue light negative phototaxis[27]. In biological environment, it shows a yellow color. It also carries the last kind of chromophore that naturally existed among the earth creatures, which is an anionic cinnamone derivative (pCA) [28]. (Please refer to fig.1.1)

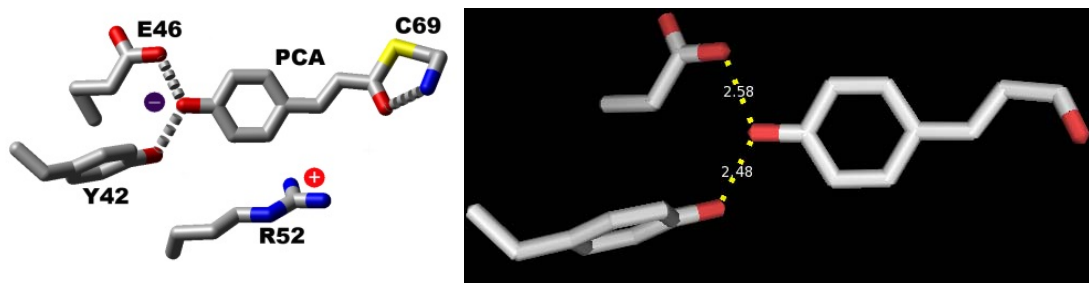


Figure 1.1 Left: Active site structure of wild type PYP(wtPYP). There are hydrogen bonds between E46 and pCA, Y42 and pCA and still another hydrogen bond formed between C69 and pCA.[29] This is generated using Molmol[30]. Right: Active site structure of wtPYP (PDB ID: 1NWZ). This is generated using Pymol[31].

The structure of active site is shown as Figure 1.1. The major hydrogen bond network is formed between three molecules: pCA, Glu46 and Tyr 42. In our simulation, we use the side chain of Tyr to represent Tyr 42 and sidechain of Tyr with one Carbon longer to represent the pCA. The Glu46 is modeled using its sidechain.

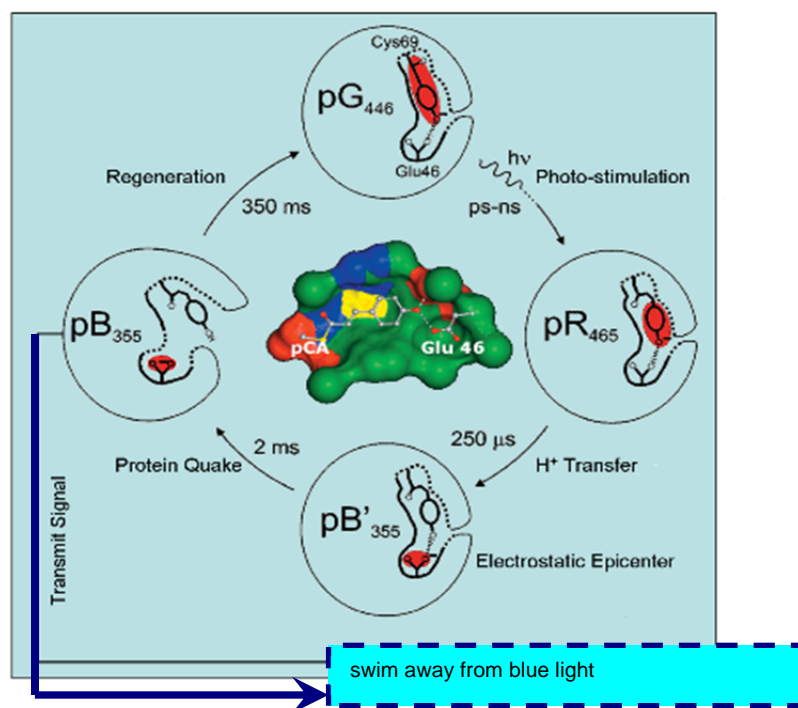


Figure 1.2 The photocycle of PYP

From the Fig. 1.2 we can see the complete photocycle of PYP. The description of major changes happened in PYP is summarized below.

First, we describe the pG to pR transition. The ground state of PYP contains pCA[-] that is buried inside the protein and stabilized by two hydrogen bonds with Glu46, Tyr42 respectively and Arg52 is also a kind of counterbalance to pCA [-]. Upon receiving a photon of blue light, the pCA[-] undergoes a conformational changes (photoisomerization) from *trans* to *cis*, therefore initiates the photocycle from Ground state pG₄₄₆(446nm is the peak absorption of PYP in pG Ground state, to Receive state pR₄₆₅. The time scale for this step is of pico-seconds. In PR state, the Glu46 is neutral (protonated) and pCA is negatively charged (deprotonated).

Second, we describe the pR to pB' transition. After triggering by blue light, the PYP goes to pR state. During the transition from pR state to pB'₃₅₅ state (Blue-shifted state, 335nm is the absorption peak), the hydrogen bond situation around pCA[-] will change. Basically the proton will be transferred from Glu46 to pCA[-] along the hydrogen bond between Tyr42 and pCA[-] and they become Glu46[-] and pCA respectively[6]. The time constant for this step is ~250μs (wild type). In pB' state, the Glu46 is deprotonated and pCA is protonated and since the time scale is very short, the protein is still kept its conformation.

Third, we describe the pB' to pB transition. From pB' state to pB₃₅₅(signaling state), the protein undergoes a “protein quake”[1], which means a large conformational change takes place. It is proposed that another protein will bind PYP in this state. Therefore the signal of “blue light received” will be sent out to downstream. The time scale of this transition is about 2 ms. In pB state, the Glu46 is deprotonated and forms Hydrogen bond with protonated pCA. Tyr42 is still not hydrogen bonded with pCA.

Forth, the pB to pG transition is summarized. From pB₃₅₅ to pG is a spontaneous process and of time ~350 ms. This relatively longer time is convenient for downstream protein to bind PYP. During this process, Glu46 back to protonated state and hydrogen bonded with deprotonated pCA. Tyr42 also forms hydrogen bond with pCA[-].

Questions and challenges

The proton transfer has two basic structural elements, the proton donor and proton acceptor. For decades, what people know is the proton will transfer from donor, which has a lower pK_a , to the acceptor, which has a higher pK_a . However, it is not clear that how proton transfers is controlled. The proton transfer pathway in proteins is first discussed by Nagle and Morowitz[32]. The idea is similar to Grotthus mechanism for proton transfer in water.

HB switch and our previous results

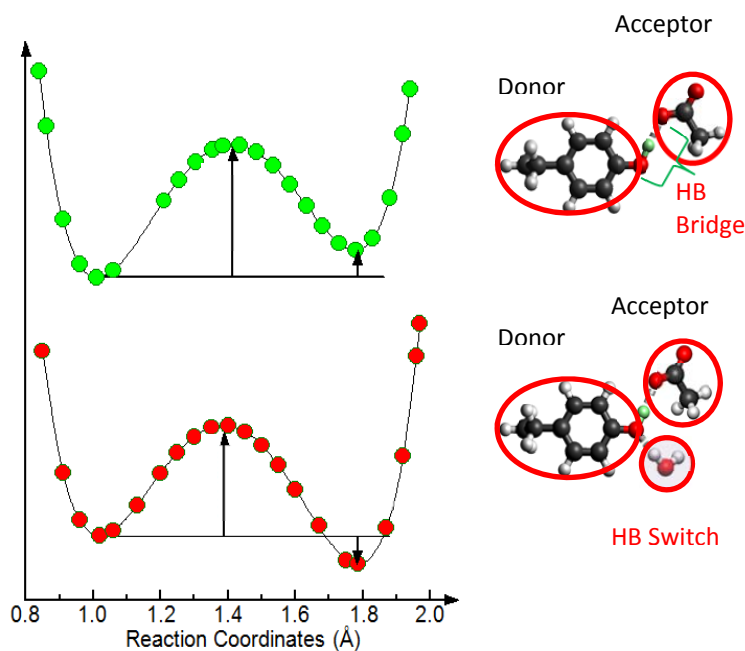


Figure 1.3 Structural elements in Proton transfer. The HB switch is H₂O molecule in this case. And hydrogen bond Bridge refers to the O...O hydrogen bond between donor and acceptor. (Adapted from Yunxing Li master thesis.)

Using quantum chemistry, the results of the proton transfer model studied previously by Edward Manda and Yunxing Li reveal role of a third structural element (or molecule), which is named HB switch. In the model, the proposed mechanism is that the hydrogen bond switch controls the direction of the proton transfer. The basic structural element for proton transfer can then be illustrated using figure 1.3.

The major conclusion is that the energy landscape in the donor side is higher than the acceptor side without HB switch. And after interaction with HB switch, the energy landscape in the acceptor side is lower. So the proton could transfer. In addition, the donor – acceptor distance, which is named HB Bridge, controls the energy barrier height between the donor and acceptor. The shorter distance will result in a lower barrier. This idea is illustrated in Figure 1.4.

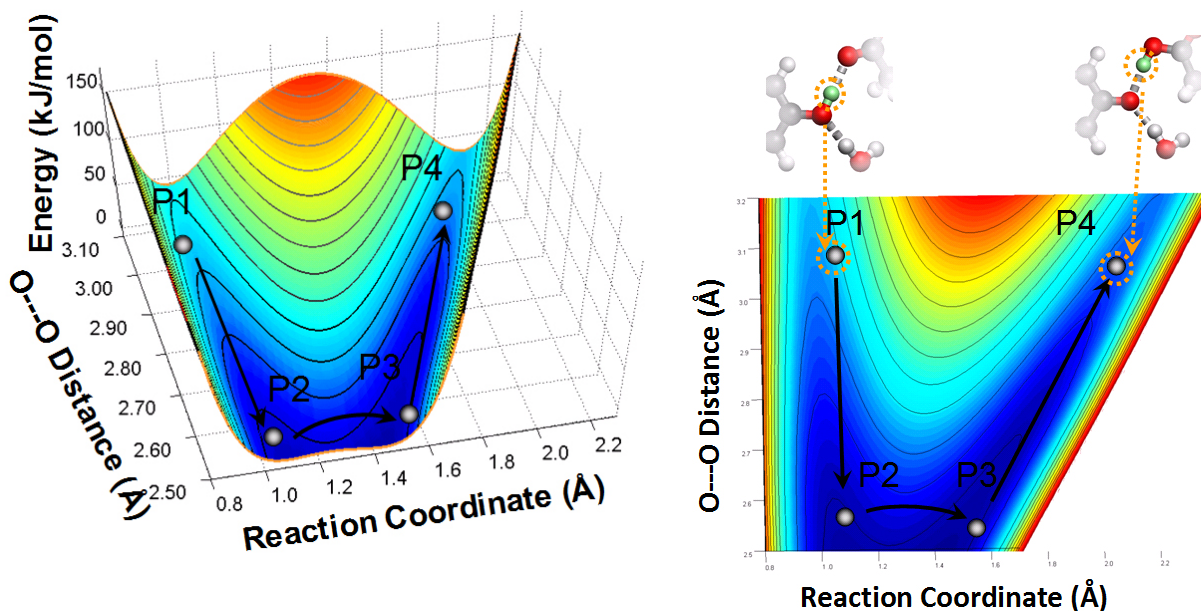


Figure 1.4 The 3D potential energy surface. (PES) The molecule of the switch is H_2O , and the distance between switch and donor is 2.80\AA . Right: mapping the position in 3D into the structural complex. P1 and P2 correspond to the positions in the structure cartoons above.

History of the research in proton transfer (our lab)

In 2006, Edward Manda, a undergraduate entering lab supported by the Niblack research scholarship, did quantum chemistry calculation using Gaussian03 to investigate the hydrogen bond effect on changing the proton affinity. The energy landscape analysis method was used to examine

the change before and after adding the HB switch. The method used was B3LYP 6-31G(d) for structure optimization and B3LYP 6-311+G(2d,p) for energy calculation. The cases investigated includes Donor-Acceptor (DA) =2.80Å (without HB switch and with H₂O as switch (Switch-Donor distance (SD)=2.80Å)); Donor-acceptor=2.60Å, 2.49Å (with H₂O as switch(SD distance=2.80Å)). He is the first to find correct energy landscape shape. In addition to this, he also explored the possibility that His [0] (DA=2.80Å, SD=2.80Å) being the switch. The calculations were also done with different dielectric environments.

After Edward graduated, Yunxing continued to work on proton transfer research and used this as her master thesis topic. First she investigate many different HB bridge distance (2.49, 2.60,2.70, 2.80, 2.90, 3.00 and 3.10Å for H₂O as the switch) and this effort result in a 3D potential energy surface. Second she explored the possibility of more molecules as the switch. This includes His[0], Gln, Tyr and Thr. And she found that different switch molecule will provide different change in proton affinity. Finally, she expanded the dielectric environment calculation to include more value. ($\epsilon=6.89$)

She also devoted much effort in plotting beautiful graphs to convey the idea of proton transfer model. Such as electron density map (without core electrons) and 3D potential energy surface map(with help of Johnny Hendriks).

Aims for this thesis:

The major goal for this thesis is to characterize the role of HB switch played in proton transfer. Because this is a brand new structural element introduced in the proton transfer field, we basically will analyze the calculation result for the following three aims.

Aim 1 is to determine the effect exerted by different ***strength*** of Hydrogen Bonds (HBs), (different switch-donor HB distance, and different donor groups), on the proton transfer group. And **Aim 2** is to determine the effect exerted by different ***type*** of the switch-donor Hydrogen Bonds, namely HB through “O...O”, “O...N” and “O...S” on the proton transfer group. **Aim 3** is to examine the effect exerted by different ***angle*** of Hydrogen Bonds (HBs), (different Switch-donor HB angle) on the proton transfer group.

Structure of the thesis:

Introduction: background information; Computational theories and method: method used in the thesis including constraints; Results and Discussion: Results from the study and discussion; Concluding remark: Conclusion

Chapter II

First Principle Computational Theories and Method Used in This Study

2.1 Atomic and Molecular Modeling (Quantum Mechanics Based)

2.1.1 Basic equation

Quantum mechanics is originated based on the idea of energy quanta, which is first put forward by Planck[33]. Many great scientists contribute to the later development of the Quantum mechanics. One of the established theories is based on the well-known Schrodinger equation, which reads:

$$H\Psi=E\Psi$$

From the Schrodinger equation, we can safely describe the system using the variable Ψ . Because the way Schrodinger equation is derived usually connect it with wave, this formulism also called wave mechanics and Ψ the wave function. The word “first principle” or “Ab Initio method” is used when we calculate the properties of the matter starting from its wave function.

Although the physical meaning of Ψ is not known at first and still many people provide different opinions on it now, the most accepted explanation is from M. Born, which is called the statistical explanation. He relates the discovery of a particle in certain region to the $|\Psi(\vec{x}, t)|^2$ or more precisely:

$$\int_a^b |\Psi(\vec{x}, t)|^2 d\vec{x} = (\text{Probability of discovering a particle in the region from } a \text{ to } b.)$$

where $|\Psi(\vec{x}, t)|^2$ is the wave function (also called probability density).

We now take the electron as an example. From the quantum mechanics point of view, the electron around the Hydrogen nucleus is not in a fix position or a narrow orbit but rather distributes in a large space (electron cloud), which is described by Ψ of the following Schrodinger equation (we just consider the steady state, meaning $\Psi = \Psi(\vec{x})$):

$$\hat{H}\psi = \left[-\frac{\hbar^2}{2m} \nabla^2 - \frac{e^2}{4\pi\epsilon_0 r} \right] \psi = E\psi ; r \text{ is the radius of hydrogen atom}$$

The bound state solution can be written as (polar coordinates used):

$$\Psi_{nlm} = R_{nl}(r)Y_{lm}(\theta);$$

The n, l and m represent the quantum state; $R_{nl}(r)$ represents the radial distribution and $Y_{lm}(\theta)$ is the angular part. They together give the description for the electron distribution around the hydrogen nucleus. Then we can introduce the concept of probability density of electron or electron density:

$$\rho(\vec{x}) = \int |\Psi(\vec{s})|^2 d\vec{s}$$

According to the postulate summarized by Von Neumann, the property of Ψ is finite, single-valued and well-behaved in first and secondary derivative. Then we have:

$\int \rho(\vec{x}) d\vec{x} = 1$ (for hydrogen atom we discussed above) or $\int \rho(\vec{x}) d\vec{x} = N$ (for N electrons system)

2.1.2 Atomic and molecular models from Quantum mechanics point of view

The underlying physical laws necessary for the mathematical theory of a large part of physics and the whole of chemistry are thus completely known, and the difficulty lies only in the fact that the exact application of these laws leads to equations much too complicated to be soluble.

Paul Adrien Maurice Dirac

As we discussed above, the problem of one electron can be attributed to solving the corresponding Schrodinger equation. In principle, we can do the same for heavy atom or molecular system, which has more than one electron and also different nuclei. But they are much more complicated.

The Born-Oppenheimer approximation allows us to separate the wave function into Nuclei part and electron part, that is $\Psi_{total} = \Psi_e \times \Psi_{Nu}$. It states that the electron movement is much faster than nuclei. So we first approximate the nuclei are fixed and therefore what electrons bear is the equivalent coulomb potential.

Now in general, if the system contains N electrons and M nuclei (same kind), then it has the Hamiltonian:

$$\hat{H} = -\frac{\hbar}{2m} \sum_{i=1}^N \nabla_{e,i}^2 + -\frac{\hbar}{2M} \sum_{j=1}^M \nabla_{Nu,j}^2 + -\sum_{i=1}^N \sum_{j=1}^M \frac{Z_A e^2}{4\pi\epsilon_0 r_{ij}} + \sum_{j=1}^M \sum_{k>j}^M \frac{Z_A Z_B e^2}{4\pi\epsilon_0 R_{jk}} \\ + \sum_{i=1}^N \sum_{l>i}^N \frac{e^2}{4\pi\epsilon_0 r_{il}}$$

Where

$$\hat{T}_e = -\frac{\hbar}{2m} \sum_{i=1}^N \nabla_{e,i}^2 \quad \text{Kinetic energy for electrons}$$

$$\hat{T}_{Nu} = -\frac{\hbar}{2M} \sum_{j=1}^M \nabla_{Nu,j}^2 \quad \text{Kinetic energy for nuclei}$$

$$\hat{V}_{Ne} = -\sum_{i=1}^N \sum_{j=1}^M \frac{Z_A e^2}{4\pi\epsilon_0 r_{ij}} \quad \text{Nuclei-electron interaction potential}$$

$$\hat{V}_{NN} = \sum_{j=1}^M \sum_{k>j}^M \frac{Z_A Z_B e^2}{4\pi\epsilon_0 R_{jk}} \quad \text{Nuclei-nuclei interaction potential}$$

$$\hat{V}_{ee} = \sum_{i=1}^N \sum_{l>i}^N \frac{e^2}{4\pi\epsilon_0 r_{il}} \quad \text{Electron-electron interaction potential}$$

And r_{ij} or R_{jk} is the distance between i and j or j and k species.

With proper approximation and modern computation power, we can solve the Schrodinger equation numerically. Here we will discuss about these Models with focus on the quantum mechanics treatment.

2.2 Density Functional Theory (DFT)

There are two possible outcomes: if the result confirms the hypothesis, then you've made a measurement. If the result is contrary to the hypothesis, then you've made a discovery.

--*Enrico Fermi*

Because of the limitation in HF model, it cannot be used in our calculation. Pondering between Post-HF method (e.g. MP2 method) and DFT method, we chose the latter because of the better cost/accuracy ratio. The following is a short introduction for this method.

1. Hohenber-Kohn theorem and Kohn-Sham equation

We will not go into the detail of the theorem[34], but rather states the result from the theorem. Basically, the Hohenber and Kohn's work is first about the existence of the functional of single electron density $\rho(\vec{x})$ in ground state that is correspondent to the many-body wave function, and second the true density has the lowest energy.

This theorem assures us that we can use single electron density instead of the wave function to explore any ground state properties. what we need is the method to seek for the correct electron density function, which is the Kohn-Sham equation provided by Kohn and Sham[35].The energy of the electrons now has the form:

$$E = E^V + E^J + E^T + E^X + E^C$$

The first term is and second term is potential energy result from the nuclei and electron. The last three, E^T , E^X and E^C are electron kinetic energy, exchange and correlation energy. The HF model has the same E^V and part of E^X , other energy terms are unique in DFT model. Depending how to deal with these unique terms, the DFT can be divided into LDA (use local density approximation), GGA (use general gradient approximation), meta GGA and Hybrid (mix of the two

approximation). Table 2-1 gives a list of typical functionals in each category. Also recently, linear scaled DFT becomes available in the software package(e.g. ONETEP[36]).

2. Comparison of the models and our choice

We now have two models, one is based on wave function (HF-LCAO) and the other is based on electron density (KS-LCAO). The HF-LCAO is approximation to the exact solution of Schrodinger equation and the accuracy can be improved by systematic effort. The KS-LCAO method uses KS equation and currently there is just approximate solution although in theory there is accurate solution. So one is approximate equation but we solved exactly, and the other is exactly equation but we solved approximately [37].

3. Functional

As its name tells, functionals play an important role in calculation scheme of DFT. By definition, functional is a map from a set of functions to the variables[38]. This idea tells us, instead of looking for the function from the variable side; we could look for the function from the functional side. The Hohenber-Kohn theorem promises the existence of such functions if we start from the functional side. And the Kohn-Sham equation provides an operational way to do so.

With the effort of many researchers, we could use most proper functional according to the system we are dealing with. The major type includes[39]: LDA(Local density approximation)[35] type, GGA(Generalized Gradient Approximation) type, meta GGA and Hybrid[40] type. In the table2.1, typical functionals are listed.

With recent development, the DFT has proved its power. Some of the new functionals (m06-2x-d3, wb97xd) yield results that are more accurate than MP2 method[41]) while the computation cost still lower than MP2.

Table 2.1 Examples for different types of functionals.

Types of Functional	Examples		
GCA	PW91[42]	PBE[43]	BLYP[44, 45]
Meta GCA	TPSS[46]		
Hybrid	B3LYP[40, 45, 47]	TPSSh [48]	

In the future, we may try other third generation functionals, e.g. MPW1B95 or MPWB1K [41, 49], but for our purpose of proof of concept study, B3LYP provide good enough result.

4. Basis sets

No matter what kind of model you choose (HF, post-HF or DFT), when you perform the real calculation work, the basis sets always need to be considered. Generally speaking, the larger basis sets you choose, the more accurate result you will have and more computation time is required. Depending on the time complexity of the algorithm, the increment in time consumption is rarely linear. There is a collection of available basis sets online at: <https://bse.pnl.gov/bse/portal>.

In the section of Hartress-Fock-Roothaan model, we discussed about the LCAO approximation, which uses linear combination of atomic orbitals to approximate the molecular orbitals. By doing this, we decomposed the molecular orbitals into the atomic orbitals. In this sense, we could call atomic orbitals the basis set for this operation. Basically, we have three type of basis sets to choose from, Slater Type Orbital (STO), Gaussian Type Orbital[50] (GTO) and augmented plane-wave (APW) or augmented spherical wave (ASW). How to choose the function form of wave function is then a question concerning the calculation accuracy and efficiency. Additionally, we already know that DFT includes correlation energy. And the correlation energy is sensitive to basis sets choice[51].

STO could correctly describe the behavior around the nucleus, but because of Gaussian product theorem, the integrals using GTO is much easier to calculate[52]. So what we usually do is to use several combination of GTO to approximate the STO (Contracted Gaussian Type Function,

CGTF). The result will depend on how many GTO we use. In this case, the GTO we used here also called primitive Gaussians.

We list here the expression of STO and GTO just in Cartesian coordinates[51].

$$\varphi(x, y, z) = Nx^a y^b z^c e^{-\zeta r} \quad \text{Slater type orbitals in Cartesian}$$

$$\varphi(x, y, z) = Nx^a y^b z^c e^{-\zeta r^2} \quad \text{Gaussian Orbitals in Cartesian}$$

When $a + b + c = 0$, it is called s-type GTO, and there is one s-type GTO in one CGTF;

When $a + b + c = 1$, it is called p-type GTO, and there are three p-type GTO in one CGTF;

$$\varphi(x, y, z) = N \sum_{i=1}^n c_i x^a y^b z^c e^{-\zeta_i r^2} \quad \text{Contracted Gaussian Type Function in Cartesian}$$

In the old literature, ζ (zeta) is used to represent the atomic orbitals. When the number of CGTF used to describe STOs is just the same as number of atomic orbitals (can be called one suit of ζ), which is a kind of minimal requirement, it is called **Minimal basis set**[51]. And **Extended Basis Sets**[53] refers to those basis sets, which use more than one set of ζ to approximate the STO. **Split valence**[51, 53] gives more CGTF for valence orbitals. **Polarization**[51, 53] means add more orbitals to the given atom.

Basis set superposition error (BSSE) mainly comes from the fact that the basis sets we use are not infinitely large. The overlap of the basis sets from molecule A and that from molecule B tend to give an additional energy, which is an artifacts depending on the size of the basis sets used. That means the energy of interaction is not just $\Delta E = E_T - E(A) - E(B)$

Generally speaking, we should consider performing BSSE correction. However, in hydrogen bond research, as long as we use relatively large basis set and add polarization then the results are much similar between with and without BSSE correction[54]. More often than not, the situation is over-corrected by using BSSE correction in weakly interacted system[9]. Also, the method used to perform BSSE in Gaussian 03 software package is Counterpoise Method (CP)[55], which is also an approximate correction and could cause additional error due to its methodology principle[9]. In our study, we used a large basis set with polarization, which will be discussed below, so we didn't perform the BSSE correction.

2.3 Method Used in This Study (DFT functional, Constraints and Potential modeling)

In this section we will describe the method for calculation and analysis. As we stated earlier this chapter, we chose the DFT method. We repeated the same reasoning here again. HF model cannot be used here. DFT is one of the best candidates, because it includes the exchange-correlation energy from the beginning. Please refer to the hydrogen bond section in chapter I for theoretical reason for this. And also the computation cost of DFT is less than MP2 (or other post-HF) method. With recent advance, the accuracy of DFT can be comparable or even better than MP2, with careful chosen of functional and basis sets[56]. Although other post-HF (e.g. QCCSD) method yields the best results, the computation cost is too expensive. The B3LYP functional, which is a combined effort from B3, LYP and VWN [58-60], is essentially a hybrid functionals. It could give results enough accurate for hydrogen bonded system (for our purpose of proof of concept study) while keeping the computation cost reasonable [57, 58]. So it is quite popularly used in the hydrogen bond and proton transfer research [59, 60]. As a reference, its E^{XC} term reads[40]:

$$E_{B3LYP}^{XC} = E_{LDA}^X + n_0(E_{HF}^X - E_{LDA}^X) + n_x(\Delta E_{B88}^X) + E_{VWN3}^C + n_c(E_{LYP}^C - E_{VWN3}^C)$$

Where in the paper[40] the coefficients are $n_0 = 0.2$; $n_x = 0.72$; $n_c = 0.81$. Those are designed to fit *He* data.

E_{LDA}^X is exchange energy from LDA; E_{HF}^X is exchange energy from HF method; ΔE_{B88}^X is exchange energy from Becke 88 functionals[44]; E_{VWN3}^C is correlation energy from VWN[47] version 3; E_{LYP}^C is the correlation energy from LYP functionals[45].

Basis set used in this study

In our calculation, the basis set we used is 6-311+G(2d,p). In this basis set, 6 CGTF are used for core electrons, and 3 additional CGTF is used for valence orbitals, which are formed by 3, 1 and 1 primitive Gaussians, respectively. Polarization is added, which is (2d,p) meaning that for heavy atom, the atomic orbitals till 2d is required and for hydrogen atom atomic orbitals till p is required. Also, from the introduction on hydrogen bond, we realize that to correct model the hydrogen bond, whose energy has polarization and diffuse part[14], we need to add basis sets that responsible for diffusion. This is achieved using “+”, which means add diffuse function to heavy atom.

Gaussian03 software package

Gaussian03[61] is a one of the most popular commercial software package designed for quantum chemistry calculation. It provides the DFT method that we needed in this study and it could also provide other calculation methods (e.g. semi-empirical method, molecular mechanics, post-HF method and ONIOM). Equipped with these methods, Gaussian03 could provide theoretical results on atoms, molecules and reactive systems for their energy, structures, charge density and vibrational frequencies.

Restricted switch donor hydrogen bond distance calculation

Density functional theory is used for whole study. All calculations are carried out by Gaussian 03[61] software package, which is installed in university HPCC (Cowboy). B3LYP functional together with 6-311+G(2d,p) basis set is applied, the meaning of which we discussed in section 2.2.

Fig2.1 shows a typical calculation in the study. We use this as an example to explain how the constraints are set. We first fix the O7-O8 distance (donor-acceptor distance) to be 2.8 Å, and O12-O7 distance (switch-donor distance) to be 2.8 Å, H15-O7 distance to be 1.4 Å. This is to perform the transition state calculation. Then we perform geometry optimization with above 3 constraints. Based on the optimized structure, we calculate the energy of the system. This is called T state (Transition state). In this proton transfer group, T state is also the transition state.

Then we read the angle 6-7-8 (number of the atom, please refer to Figure 2.1) and angle 6-7-12 from the C state. After manually moving the H15 to the O7 side (Donor state or D state) or to the O8 side (Acceptor state or A state), we again perform the geometry optimization under the constraints of “O7-O8=2.8 Å”, “O12-O7=2.8 Å”, “6-7-8=angle from T state” and “6-7-12=angle from T state” for the D and A state respectively. Then energy of the optimized structure is calculated. This is to acquire the energy for D state (proton with O7) and A state (proton with O8). Then we can calculate for energy barrier for this reaction, which is given by $E(T)-E(D)$ and proton affinity, which is given by $E(A)-E(D)$.

We then repeatedly perform this calculation for different O7..O8 distance and O12...O7 distance and different donor-acceptor molecules.

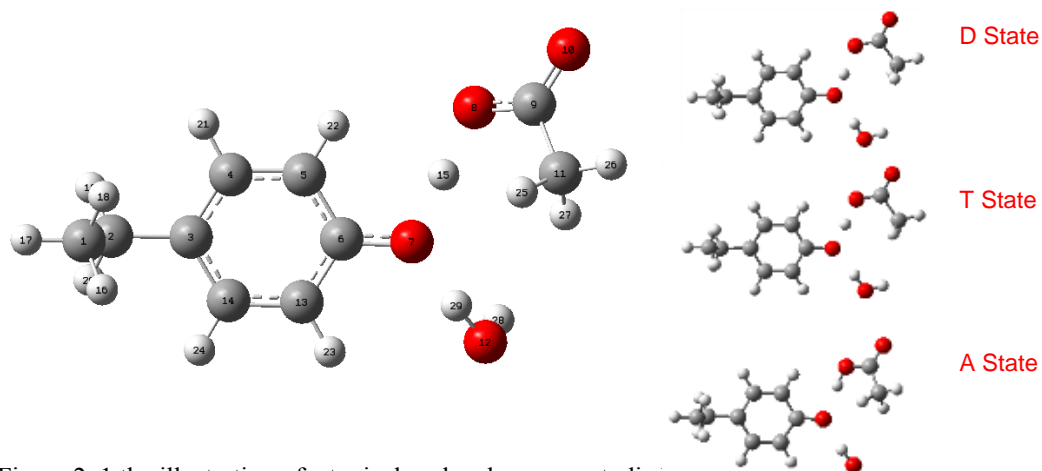


Figure 2. 1 the illustration of a typical molecular group studied.

Free switch donor hydrogen bond distance calculation

In this calculation, the T state is acquired with the constraints of $O7...O8=2.80\text{\AA}$ and $O7...H15=1.40\text{\AA}$. The distance of $O7...O12$ is free. Then we read the angle of 6-7-8 (number of the atom, please refer to Figure 2-1) and angle of 6-7-12 from the T state. In the D and A state calculation, the constraints are $O7...O8=2.80\text{\AA}$, the angle of 6-7-8 and angle of 6-7-12. After finishing all calculation on D, T and A state, we then calculate the energy barrier ($E(T)-E(D)$) and proton affinity ($E(A)-E(D)$).

Angle scan calculation

In this calculation the T state is acquired using the same constraints as the “restricted switch donor hydrogen bond distance calculation”. Then in D (or A) state calculation, we keep the following 3 constraints the same: donor-acceptor distance, switch-donor distance and angle 6-7-8, while the fourth constraints, we use a series of value (from 110° to 140° with stepsize 5°) to construct a series of calculation.

Dielectric constant calculation

In order to approximate the environment inside protein better, we also carried out the calculation in dielectric constant environment. According to a related review [62], although the choices of ϵ are different from literature, overall the dielectric constant inside the protein is much lower than water ($\epsilon=80$). Among all the values, $\epsilon=4$ is frequently used by researchers[63]. In this study, to calculate the energy in dielectric medium, we use Polarizable continuum (PCM) model which is implemented in G03 software. This model is developed first by Tomasi and coworkers [64, 65].

Morse potential modeling

The most used potential to model the diatomic disassociation or ionization is Morse potential[66], which has the following form:

$$E(r) = E_1 \cdot (1 - e^{-a(r-r_1)})^2 + E_0$$

The fitting parameters are: E_0, E_1, r_1 and a .

The physical meanings[66] of E_1 is the minimums energy achieved at $r = r_1$. If we use k to denote the force constant of the chemical bond, then we have $a = \sqrt{\frac{k}{2E_1}}$.

In quantum physics, it also used as one kinds of aharmonic potentials because it has the advantage of having analytical solutions[66, 67]:

$$\varphi_n^v(y) = N_n^v e^{-\frac{y}{2}} y^s L_n^{2s}(y)$$

Where:

N_n^v is normalization factors;

$L_n^{2s}(y)$ is Laguerre functions and y is related to the r by $y = ve^{-ar}$

The energy levels are given by

$$E = -E_1 + \hbar\omega_0 \left(n + \frac{1}{2} \right) - \left(\frac{\hbar^2 \omega_0^2}{4E_1} \right) \left(n + \frac{1}{2} \right)^2 + E_0$$

The typical Morse Potential is shown as Figure 2.2.

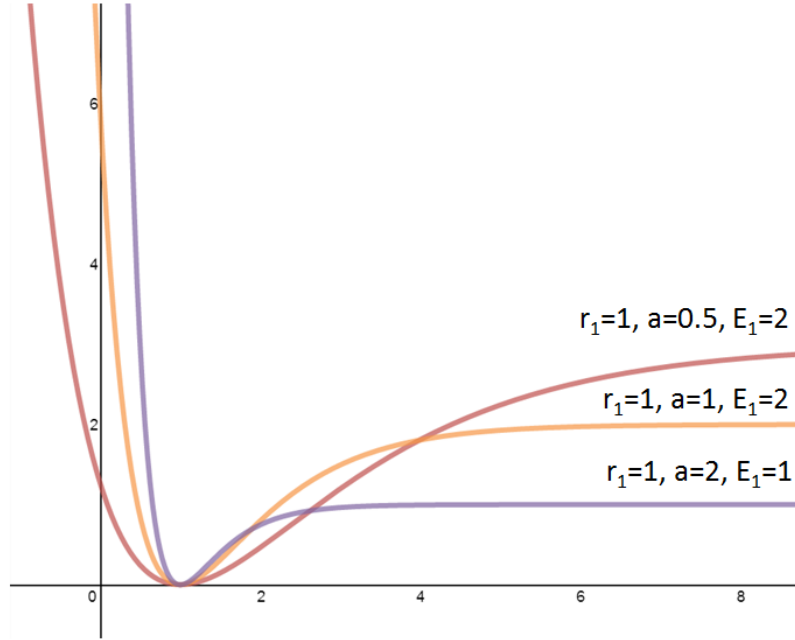


Figure 2. 2 Morse potential curves.

The Morse potential curves were plotted with different parameters in the Figure 2.2. From mathematics' point of view, the parameter “a” controls the behavior of the curve approaching asymptotes when r is larger than r_1 . If the atom is placed at the origin, the curve could penetrate into the core region with proper value of “a”. However, this is not right from physics point of view, where proton cannot penetrate into heavy atom.

And the potential to model the donor-acceptor interaction is double Morse potential, which has the following form:

$$E(r) = E_1 \cdot (1 - e^{-a(r-r_1)})^2 + E_2 \cdot (1 - e^{-a(r-r_2)})^2 + E_0$$

The fitting parameters are: E_0, E_1, E_2, r_1 and r_2 .

The physical meanings of the above parameters are similar to single Morse potential.

Lennard-Jones Potential modeling

The most used potential to model the interaction between neutral molecules is Lennard-Jones potential:

$$E(r) = E_1 \cdot \left(\left(\frac{r_0}{r} \right)^{12} - 2 \left(\frac{r_0}{r} \right)^6 \right) + E_0$$

The fitting parameters are: E_0, E_1, r_0

The physical meanings of E_1 is the energy minimum achieved when r is equal to r_0 . The typical L-J potential curves are shown in Figure 2.3.

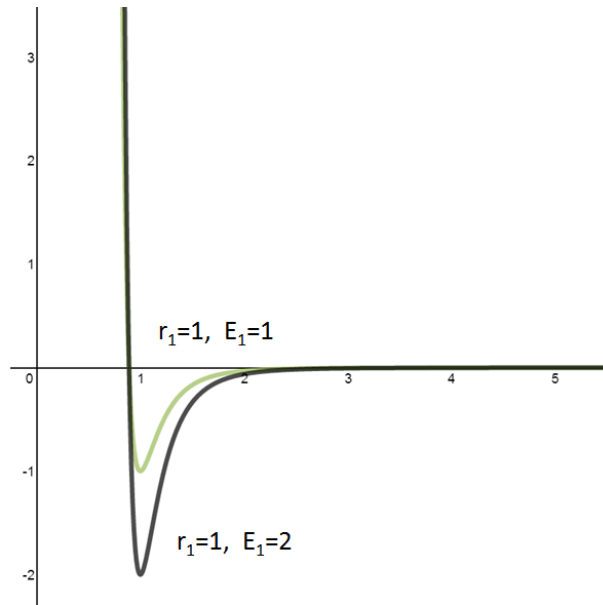


Figure 2. 3 Lennard-Jones potential curves.

The Lennard-Jones potential is commonly used by many molecular dynamic simulation programs, GROMOS[68], CHARMM[69]. The potential function also called “Lennard-Jones 12-6” function. Because the performance of r^{-12} is growing too fast, researchers used other form to

substitute this term, e.g. $e^{-\frac{r_0}{r}}$. There are other modified function forms designed to improve the behavior of the function in repulsive region.

CHAPTER III

IMPACT OF HYDROGEN BOND SWITCH ON PROTON TRANSFER

The purpose of computing is insight not numbers.

--Richard Hamming

3.1 Geometry and Energy Landscape Analysis

According to our proton transfer model, the hydrogen bond switch (HB switch) is a new structural element, which is used to control the direction of proton transfer. In order to model the behavior of the hydrogen bond switch in detail during the proton transfer, we designed and performed a series of quantum calculations with different geometry constraints. Our calculation was first carried out with water molecule as the hydrogen bond switch. Then the properties of other molecules that could form a hydrogen bond with the proton donor were also explored. The candidates of hydrogen bond switch are from Table 1.3 in chapter I. Then, these calculations were compared with the experimental data (e.g. crystal structures) from Photoactive Yellow Protein(PYP).

3.1.1 Switch donor hydrogen bond distance

Restricted switch donor hydrogen bond distance

Because we are modeling the proton transfer in proteins, the input structures were constructed in a way to reflect the dynamic nature of proteins. Please refer to “restricted switch donor hydrogen bond distance calculation” subsection 2.3 in chapter II for the detail of the method, including how we set constraints to input structure. From Table 3.1 to Table 3.3 are results from the output of the calculation. In these tables, the proton affinity (PA) is calculated as the Energy difference of Acceptor state (A state) and Donor state (D state).

Table 3.1 Proton affinity for different DA distances. (No switch) (The previous results are calculated by Yunxing.)

Donor-Acceptor distance(Å)	2.60	2.70	2.80
Proton Affinity (No switch) kJ/mol	8.4	9.9	11.2

Table 3. 2 Proton affinity for different DA distance. H₂O is the hydrogen bond switch. (The previous results of SD=2.80Å for DA=2.60, 2.70 and 2.80Å were first calculated by Yunxing.)

Switch-Donor distance (Å)	Donor-Acceptor distance=2.60Å	Donor-Acceptor distance=2.70Å	Donor-Acceptor distance=2.80Å
2.50	-16.0	-19.6	-22.3
2.60	-12.8	-15.9	-18.1
2.70	-10.2	-12.7	-14.3
2.80	-8.8	-8.9	-10.5
2.90	-5.4	-6.3	-7.5
3.00		-4.5	-3.6
3.20		-3.2	0.5
3.40		2.9	3.8

Table 3. 3 Proton affinity for different DA distance. Tyr is hydrogen bond switch. (The previous result of SD=2.80Å and DA=2.80Å case was first calculated by Yunxing Li.)

Switch-Donor distance(Å)	Donor-Acceptor distance=2.80Å
2.50	-33.8
2.60	-27.9
2.70	-23.5
2.80	-19.9
2.90	-16.6
3.00	-14.0
3.20	-10.0
3.40	-7.2

Table 3.1, 3.2 and 3.3 show that the shorter the switch-donor hydrogen bond length is, the larger the absolute value of proton affinity is (energy difference between A and D state). We define the switch power to describe the ability of a hydrogen bond switch to tune the energy surface.

$$E_{switch\ power} = |E_{PA\ without\ switch}| + |E_{PA\ with\ switch}|$$

When the switch-donor hydrogen bond length becomes shorter, the hydrogen bond interaction between switch and donor is stronger. Then as expected, the switch power carried by the switch molecule is also increased. This is shown in Figure 3.1.

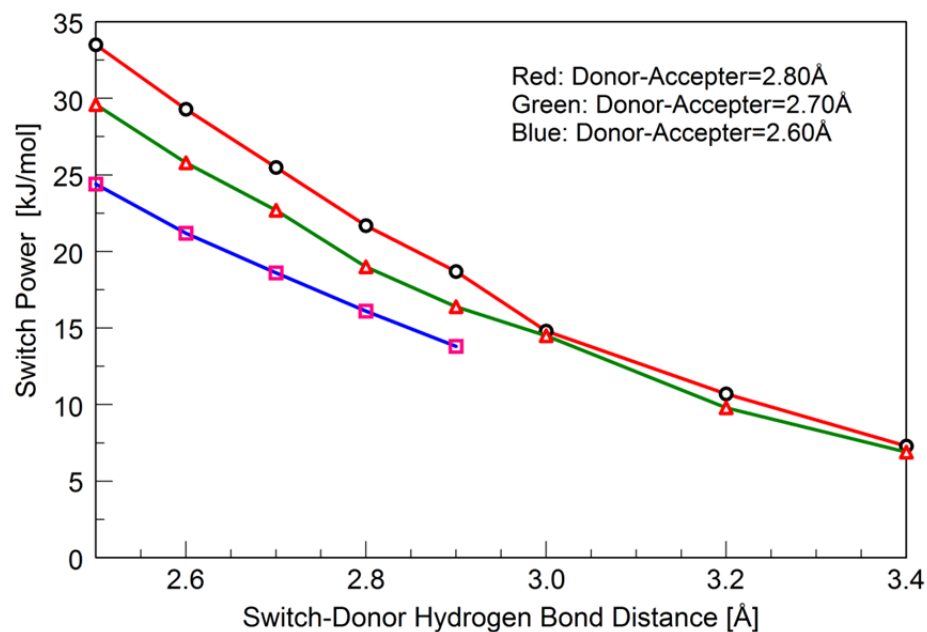


Figure 3.1 Switch power of different switch-donor hydrogen bond length (Red: 2.80Å, Green:2.70Å, Blue:2.60Å).All the calculation carried out with $\epsilon=1$.

Free switch-Donor hydrogen bond distance

In this calculation, there is no distance constraint between donor and hydrogen bond switch. Only the constraints set donor-accepter distance, donor-accepter angle and switch-donor angle are retained. (Refer to chapter II “Free switch-Donor hydrogen bond distance” section for detailed methods.)

Table 3.4 Hydrogen bond energy in D state and the switch power. The donor-accepter distances are 2.80Å and switch donor distance is free. Dielectric environment is vacuum.

	H ₂ O	Gln	Tyr
HB Energy (D state) (kJ/mol)	36.2	45.1	50.5
Switch Power (kJ/mol)	22.7	27.6	33.9

Table 3.4 shows the hydrogen bond energy for the different hydrogen bond switch with same donor-accepter distance. Because the switch-donor distance is free, it will not include the

energy from improper constraints. **And we find that the higher energy the switch-donor hydrogen bond has, the more switch power the hydrogen bond switch could provide (Conclusion 1).**

Table 3.5 Length of hydrogen bond between hydrogen bond switch and proton. There is no distance constraint between hydrogen bond switch and donor.

Hydrogen bond switch	Donor-Acceptor Distance 2.80 Å			Donor-Acceptor Distance 2.60 Å	
	H ₂ O	Tyr	Ser	H ₂ O	Tyr
switch donor distance (D state)	2.87 Å	2.82 Å	2.86 Å	2.84 Å	2.77 Å
switch donor distance (T state)	2.76 Å	2.65 Å	2.75 Å	2.76 Å	2.65 Å
switch donor distance (A state)	2.67 Å	2.55 Å	2.66 Å	2.68 Å	2.57 Å

Firstly, the data of Tyr in Table 3.5 show that when $DA=2.60\text{Å}$, the length of switch-donor hydrogen bond is $SD=2.57\text{Å}$ (A state) and the length of hydrogen bond is $SD=2.77\text{Å}$ (B state). Because these are the ideal length for Switch-Donor hydrogen bond length, it means at this distance the switch does not carry any tension forces or excess energy with it. From the active site structure of PYP (Figure 1-1), we learnt that in pG state (corresponding to A state here), the switch-donor hydrogen bond length is around 2.5Å and donor-acceptor hydrogen bond length is around 2.6Å . These values are very close to our calculation result. So our calculations indicate that in pG state of PYP, the binding pocket is relatively relaxed. However, when the proton is with pCA (corresponds to D state here), as our number shows, the ideal switch donor hydrogen bond length is 2.77Å . This value is longer than that from crystal structure. This means without other changes, the effect of proton motion on three molecules favors a structural change.

In the calculations from the last two sections, we mainly investigate the effect of hydrogen bond distance on switch power. In the next section, we will look into the effect of hydrogen bond angle on switch power. And the constraints will be changed accordingly.

3.1.2 Switch-Donor hydrogen bond angle

In this section, we are going to determine the effect of switch-donor HB angle on proton transfer. The detail of calculation methods and steps are described in the section of “switch-donor hydrogen bond angle scan” in the chapter II.

The results of angle scan are shown in the Figure 3.2. From the results we find that the energy changes as the switch donor hydrogen bond angle varies. For D state, the angle is 134.2° and for A state the angle is 123.2° . The two minimums are not achieved at the same angle, because the donor and acceptor are two different molecules, which destroy the symmetry in the plane.

From the angle scan data, we then calculate the energy difference of (A-D), which corresponds to the proton affinity. Then from the definition of switch power, we can determine the switch power for each angle and compare them. The graph is shown in Figure 3.3.

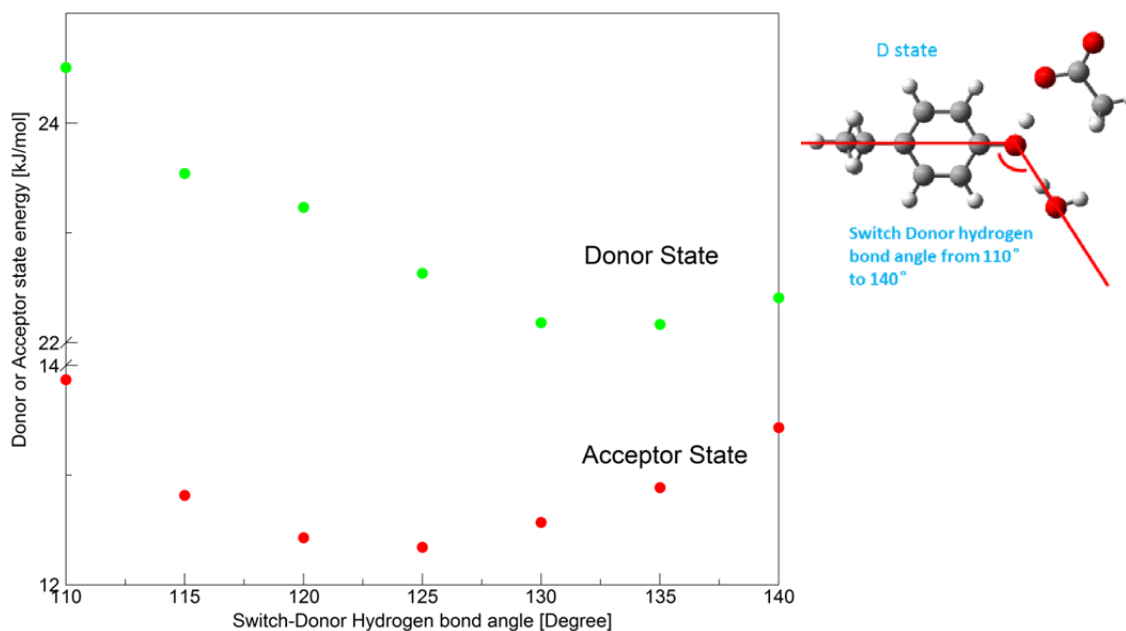


Figure 3.2 The switch-donor hydrogen bond angle scan results (with donor-acceptor distance= 2.80\AA and switch-donor distance= 2.80\AA). Green dot represent Donor state (D state) and Red dots represent Acceptor state (A state). The minimum of the curve are 134.2° (D state) and 123.2° (A state), respectively.

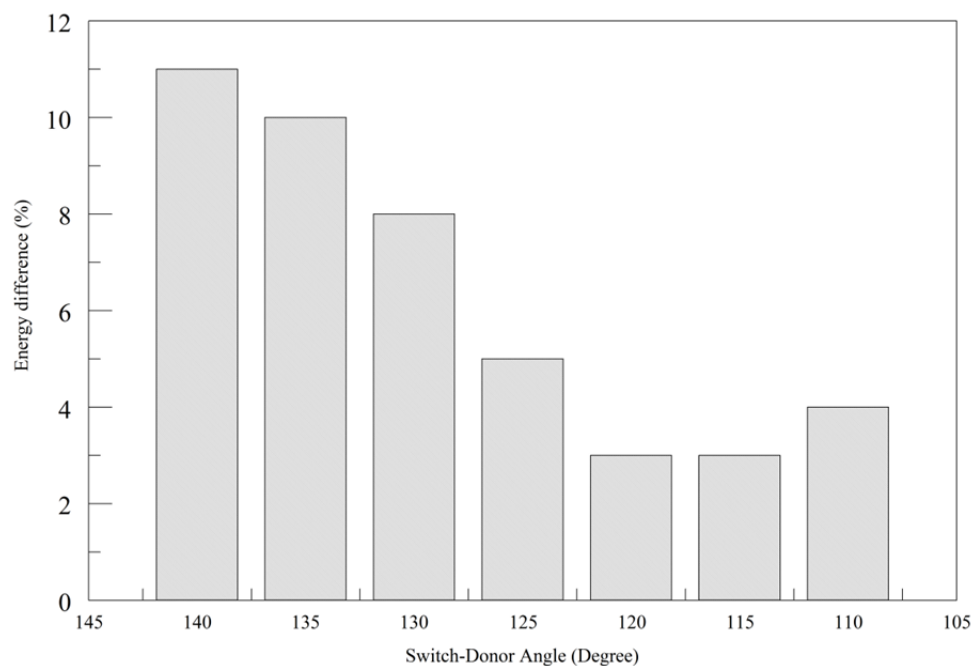


Figure 3.3 Histogram of the energy variation when angle changes from 100° to 140°

From the figure 3.3, we find that switch power varies with the switch-donor hydrogen bond angle. (Recall that the switch power is related to energy difference of (A-D).) This lead to the fact that when $DA=2.80\text{\AA}$ and $SD=2.80\text{\AA}$, the maximum of the variation is about 10% and it is achieved in A state (proton with acceptor). The angle change induced energy variation is smaller than that by distance change.

Also, the change is not symmetric with a sharper increment on the Glu side. Comparing angle change in Figure 3.2, we find that the minimum energy is always achieved at the side closer to the negative charge. For example, when the minimum energy is in B state, the negative charge is at Glu. The corresponding angle is 134.2° , which make H_2O more close to the negative charge. We then understand the symmetry broken in the Figure 3.3 is because there is net charge transferring in between two different molecules.

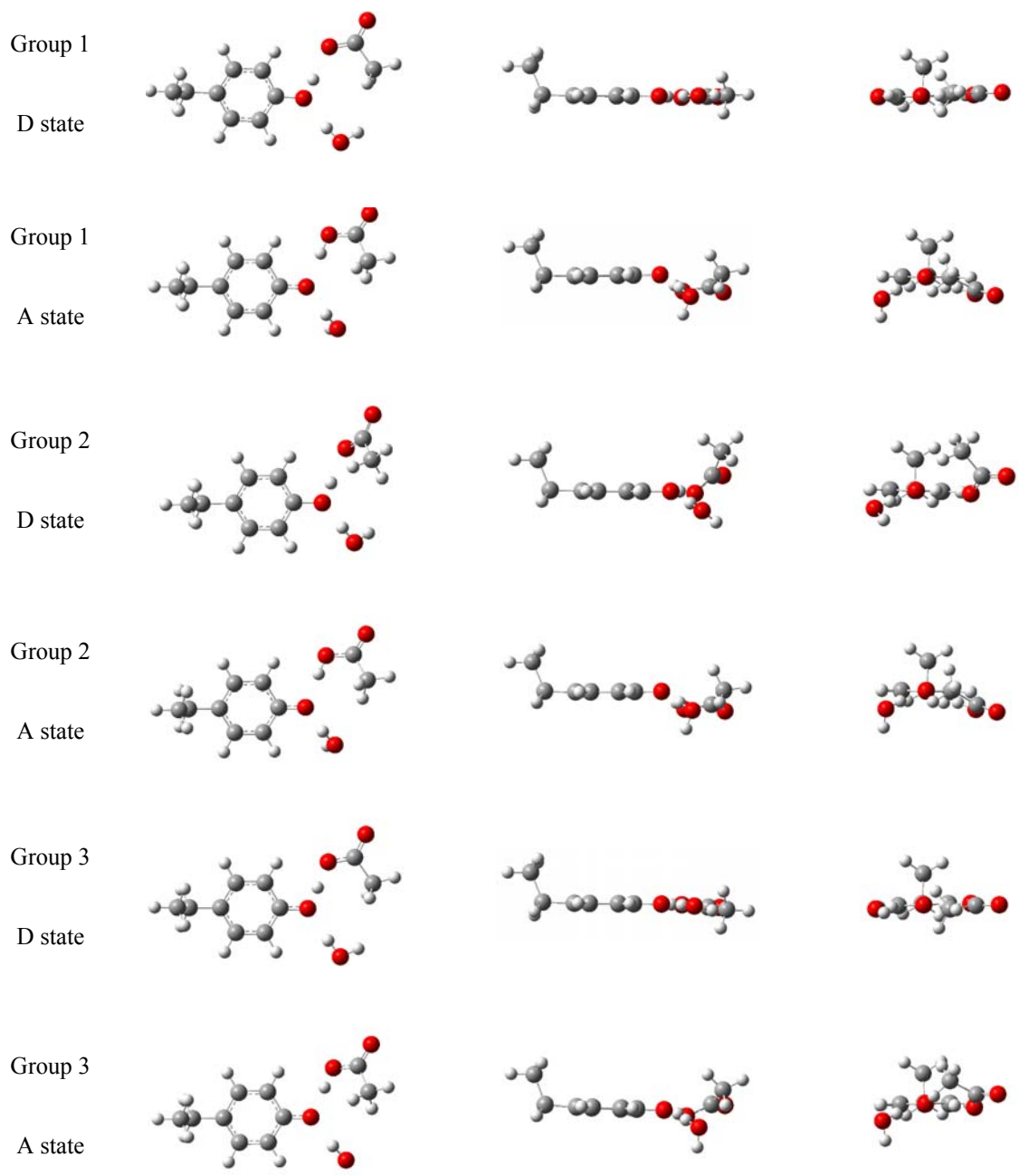


Figure 3. 4 Comparison of molecular conformation at D and A state. Group 1 (donor-acceptor distance is 2.80Å and switch-donor distance is 2.80Å), Group 2 (donor-acceptor distance is 2.80Å and switch-donor distance is 2.60Å) and Group 3 (donor-acceptor distance is 2.60Å and switch-donor distance is 2.80Å)

We further analyzed the results by looking into the conformational change. This can be visualized in figure 3.4. In the first row of Figure 3.4 (group 1 D state), where the proton is with donor, the hydrogen bond network is mostly in-plane conformation. In the second row (group 1 A state), where the proton is with acceptor, the hydrogen bond network is clearly out-of-plane. Moreover, if we compare the conformation of the complex with the same donor-acceptor distance but a different switch-donor distance, as the row 1 and row 3 showed, their conformation is quite different. However, if we compare the conformation of the complex with same switch-donor distance but a different donor-acceptor distance, as the row 1 and row 5 showed, the conformation is quite similar. The two contrasting results imply that when switch-donor distance changes, the D state conformation will change. So switch-donor distance is the factor that controls D state conformation.

Interestingly, although D state conformations are different among different switch-donor distances, the A state conformation stays similar. This indicates that, instead of going from D to A, if the system evolves from A to D, it could have the same initial structure (ground state) but end up with a quite different final conformation, depending on the switch distance it uses. This is just the case in PYP, where the active site evolves from D to B and end up with a large conformational change (protein quake).

The idea can be concluded as: upon proton transfer, there will be large molecular re-organization happen between B and D state. And the HB switch with different HB strength could lead to different degree of conformation change.

3.1.3 Switch donor energy landscape

The Morse potential fitted energy landscapes where donor-acceptor distance is 2.80 Å, are shown in Figure 3.5. And Lennard-Jones potential fitted energy landscapes are shown as Figure 3.6

and Figure 3.7. The potential function form is introduced in method section in Chapter II. PSI Plot software is used to fit the data with the two potential functions respectively.

Table 3.6 Energy barrier with different HB Bridge lengths without hydrogen bond switch.

DA distance (Å)	2.60	2.70	2.80
Energy barrier (kJ/mol)	16.5	30.3	47.2

Table 3.7 Energy barrier with the different donor-acceptor and switch-donor distance.

Switch-donor distance (Å)	Energy Barrier (kJ/mol)		
	DA=2.60Å	DA=2.70Å	DA=2.80Å
2.50	5.0	16.3	31.2
2.60	6.5	18.1	33.4
2.70	7.7	19.6	35.2
2.80	9.2	21.7	37.8
2.90	10.3	23.1	39.0
3.00		24.1	40.9
3.20		26.6	43.0
3.40		27.9	44.5

Table 3.8 Energy barrier and Proton affinity in the different switch-donor or donor-acceptor distance.

Donor-Acceptor distance (Å)	Energy barrier(kJ/mol) (H ₂ O as the switch and switch-donor distance=2.80 Å)	Proton Affinity(kJ/mol) (HOH as the switch and switch-donor distance=2.80)
2.60	14.3	-3.8
2.70	21.7	-9.1
2.80	37.8	-10.5

These calculations of different SD distance enable us to compare the effect of switch with different distances. These results consolidate one of the conclusions from previous proton transfer study in our lab: “The HB bridge length determines the proton transfer barrier and HB switch determines the proton affinity in proton transfer.” Here we support this idea with quantitative results.

First, if we maintain DA =2.80Å the same, then 0.10Å increment in SD distance would result in 1-2kJ/mol in Energy barrier but 4 kJ/mol in Proton Affinity. This is shown in the fourth column in Table3.7.

However, If we maintain SD =2.80Å the same, then 0.1Å increment in DA distance would result in 7.4kJ/mol increment in barrier height (when donor-acceptor distance increased from 2.60Å to 2.70Å), or a 16.1 kJ/mol in barrier height (when donor-acceptor distance increased from 2.70Å to 2.80Å). This switch-donor distance change will have an effect of 1.4 kJ/mol on proton affinity. This is summarized in Table 3.9.

From these quantitative results, we find that donor-acceptor distance (HB bridge) affects energy barrier more but switch-donor distance affects proton affinity more.

Table 3. 9 Energy variations when donor-acceptor (DA) or swith-donor (SD) distances changes.

	ΔE of 0.10Å change in switch-donor distance (kJ/mol)	ΔE of 0.10Å change in switch-donor distance (kJ/mol)	Conclusion
Energy barrier	7.4 or 16.1	1~2	DA distance weighs more.
Proton affinity	1.4	4	SD distance weighs more

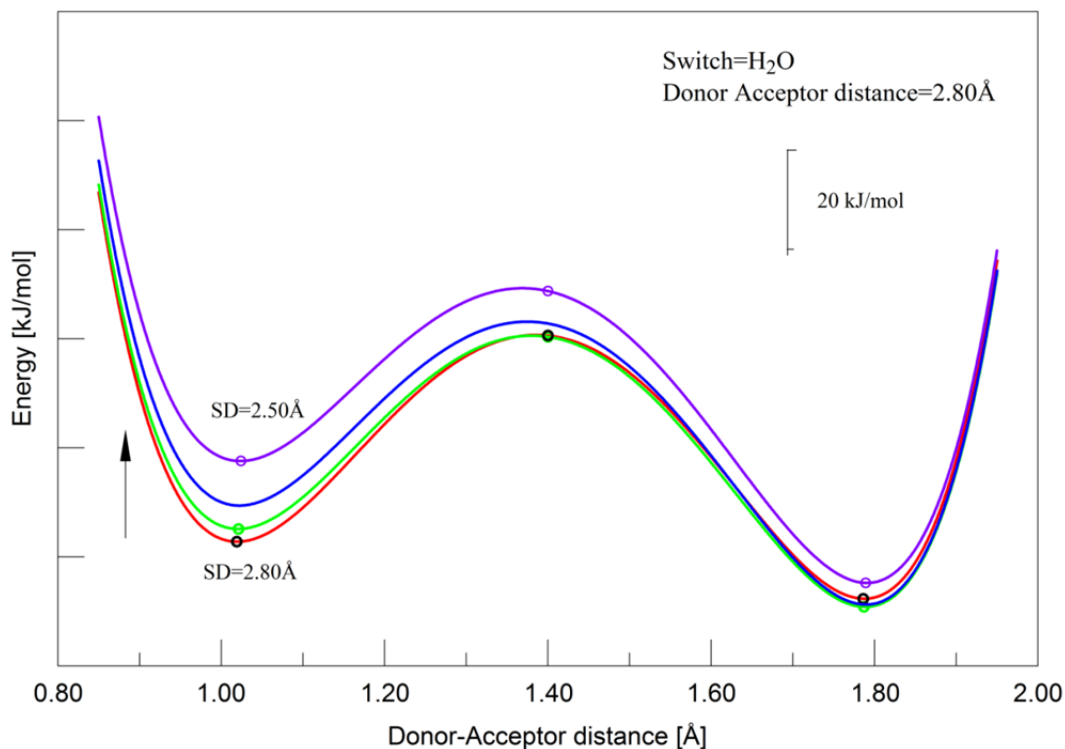


Figure 3.5 Morse potential fitting of Energy landscape for different switch-donor distance. The donor-acceptor distance is fixed to 2.80Å. Purple, Red, Green and Black are for SD=2.50Å, 2.60Å and 2.70Å and 2.80Å respectively. The circles represent the calculated data points.

Next, we will look into how the switch tunes the energy landscape to “inversed”. The potential energy landscape between donor and acceptor follows the Morse potential (Figure 3.5), which is used to describe the diatomic molecule’s ionization. The good agreement between the result and fitting suggests the hydrogen bond between Donor and Acceptor is somehow carries the feature of electrostatic. However, the hydrogen bond between switch and donor doesn’t have this property.

As Figure 3.5 reveals, the two minimums in energy landscape changes according to the variation in the switch-donor distance. The minimum to the right, which corresponds to acceptor side has limited changes (when switch-donor distance within 2.50-2.80Å). But the minimum to the left decreases as switch-donor distance increases. This different behavior suggests the mechanism

of switch tuning the energy landscape when switch-donor distance is within 2.50~2.80Å. The finding is It is the energy of donor side levels up than before (when there is no switch), as HB switch approaching to the donor (2.50Å~2.80Å). In this way, the energy landscape is inverted. And finally, because the energy in donor side levels up, the proton then will be attracted from the donor to acceptor side.

However, if the switch-donor distance is in the range of 2.80Å~3.00Å, then in contrast to the above result, the energy of the acceptor side change much more than donor side. This is shown in Figure 3.6. The two Figures (Figure3.5 and Figure3.6) suggest the way that hydrogen bond switch tunes the energy landscape is first decrease the energy minimum in the acceptor side and then increase the energy minimum in the donor side. The overall effect is the energy landscape reversed compared with no hydrogen bond switch situation.

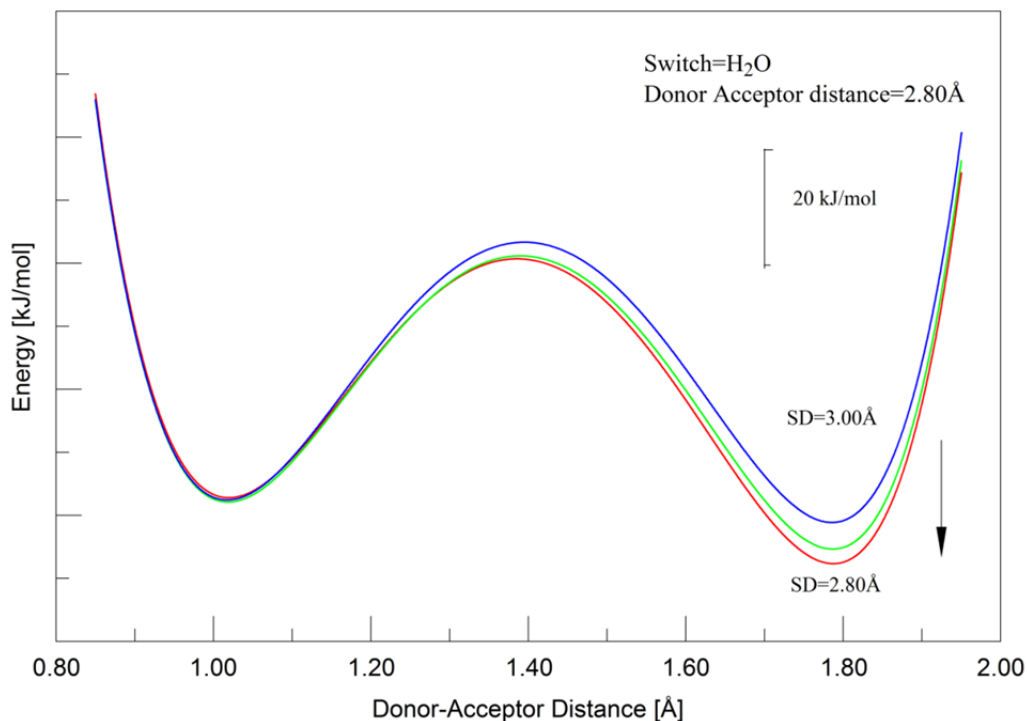


Figure 3.5 Energy landscape of the system when H₂O is hydrogen bond switch. The donor-acceptor distance is 2.80Å. Red, Green and Blue represent the switch-donor distance 2.80,2.90 and 3.00Å, respectively.

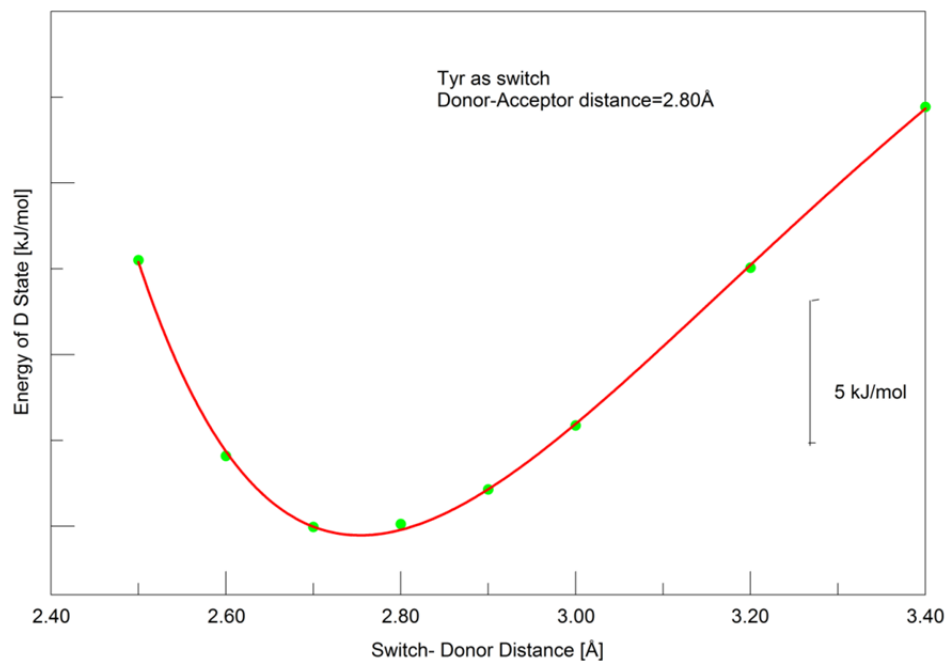
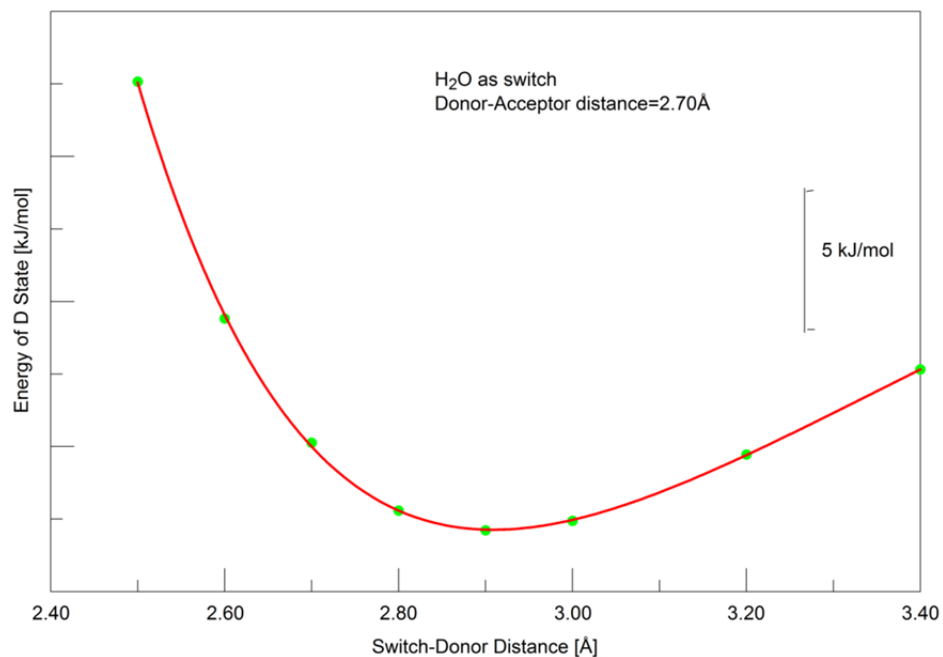


Figure 3.7 Single Morse fitting to D state energy. Upper Panel: H₂O as hydrogen bond switch and donor-acceptor distance is 2.70Å; Lower Panel: Tyr as hydrogen bond switch and donor-acceptor distance is 2.80Å.

Figure 3.7 shows the single Morse fitting of the absolute energy for D state. However, if we plot the overall energy changes of the system according to the switch-donor distance change, it can

be fitted by Lennard-Jones potential. Figure 3.8 (Tyr as switch) and Figure 3.9(H₂O as switch) are Lennard-Jones (LJ) potential fittings applied to Proton Affinity and switch-donor distance curve.

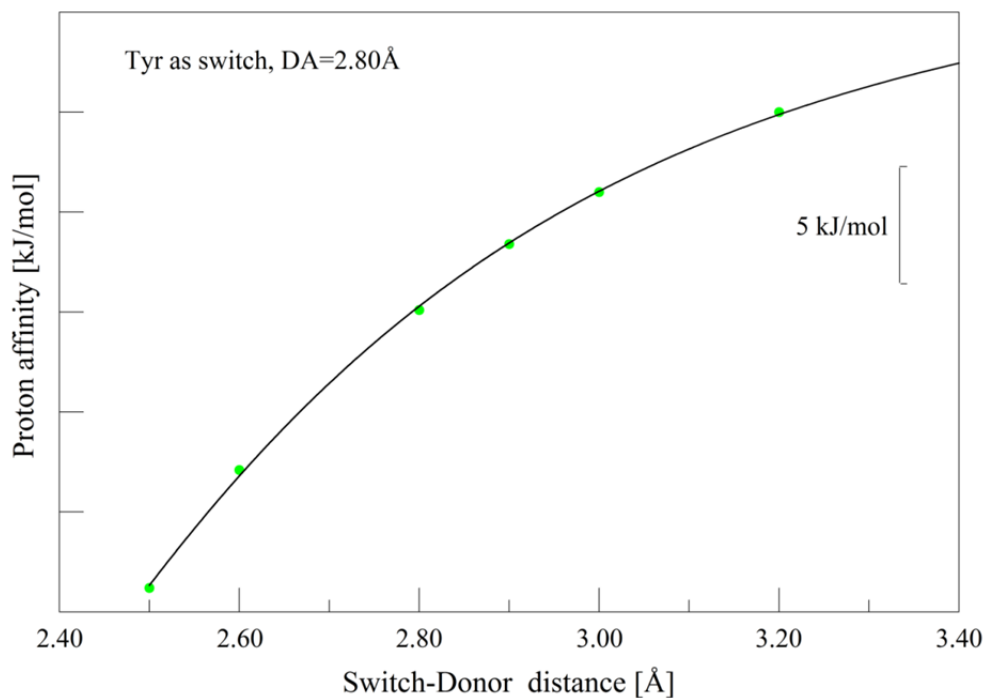


Figure 3.8 Lennard-Jones potential fit to the Energy landscape of switch-donor distance. The hydrogen bond switch is Tyr and the donor-acceptor distance is fixed to 2.80Å.

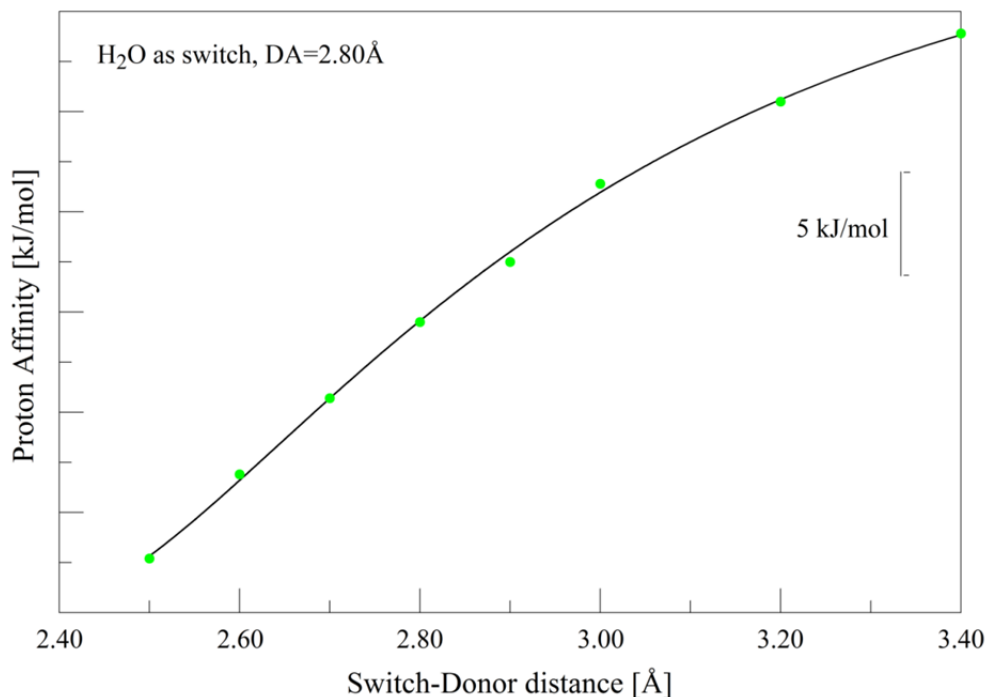


Figure 3.9 Lennard-Jones potential fitting to the energy landscape of different switch-donor distances. The hydrogen bond switch is H₂O and the donor-acceptor distance is fixed to 2.80Å.

3.1.4 Different heavy atoms in the switch donor HB and further questions

As we summarized, the switch power is determined by the hydrogen bond between switch-donor. In this section, we are going to discuss the hydrogen bond that formed with different heavy atoms (other than “O...O”).

In proteins, there are also other heavy atoms (e.g. N from His, S from Cys) that could form a hydrogen bond with the donor. The goal for this section is to examine these possibilities. We compared two molecules of similar structures. The calculation method is the same as the restricted distance calculation which describe in Chapter II. The structures of the two hydrogen bond switch were shown in Figure3.10.



Figure 3.10 Structure of two hydrogen bond switch molecules. The left one is Cysteine and right one is Serine. The yellow atom represents the Sulfur.

The switch donor distance is fixed to 2.80Å, in this case we compare the proton position between switch and donor. The results are shown in Table 3.10.

Table 3.10 Comparison of the change in bond length upon before and after proton transfer.

Switch	Serine (Ser)			Cystein (Cys)		
	Free molecule	After PT D state	Bond length change	Free molecule	After PT D state	Bond length change
Switch...H distance	0.96	0.99	3%	1.33	1.49	12%

From the table 3.10, we can find after proton transfer the bond length of Cys is longer by 12%, which is more apparent than Ser does. This is partly because the Sulfur has less electronegativity than Oxygen. And when they formed hydrogen bond, the hydrogen may deviate toward the side that has more electronegativity, which is Oxygen side in this case. However, there is another reason. This bond length change is actually a reflection of electron structure change. Because the proton is much more sensitive to the change in electron density, so the position change gives a hint to the electron density change. And also because the sulfur has less electronegativity, meaning the ability to hold electron is less, so the electron cloud change is more apparent in the case of sulfur.

This raises an interesting question, why the proton in the switch doesn't transfer to the donor. One answer from chemistry point of view is the switch group is non-ionizable or the pK_a is not lower than donor. However, there is certain occasion that we do want the proton transfer

happened between the switch and donor. And in that case we could achieve proton relay or proton translocation, which is the famous protein Bacteriorhodopsin does. Then in that case, the nature showed us her design: use a water molecule in between the donor (bR).

Further questions

The first question is why proton will transfer. By investigating the calculation results so far, we understand the answer is ultimately related to the change in electronic structure. When HB switch interacts with donor, the electron cloud is changed. Then as switch coming closer to the donor, the electron cloud is more deformed. It is the energy of donor side level up that makes the energy landscape inversed.

Because as we summarized, the proton to transfer needs two conditions: first is energy landscape inverse with acceptor side lower than donor side and we know that one way to achieve this is using Hydrogen bond to “attack” the donor.(Section 3.2.1) The second conditions is lower the energy barrier to increase the transferred population and one way to achieve the second is bring the donor and acceptor together.(Section 3.2.1) The details of how the two criteria could be met need electrostatic analysis, which we offered in section 3.2.1. For now we just believe these two ways could work.

The picture that brings donor and acceptor together to decrease the energy barrier can be vividly considered as bridge that temporally connects the donor and acceptor. The example is low barrier hydrogen bond (LBHB) in PYP between pCA and Glu46.

Second question to consider is: are there other ways to achieve these two criteria? One answer that nature provides is electron coupled proton transfer. In that case, one electron transfers first to help proton transfer (lowering the barrier) and when electron reach the destination, the potential there will be automatically lowered. This scenario can be considered as a boat that carries the proton to the acceptor and in this case the donor and acceptor are not connected directly.

3.2 Electronic structure and dielectric environment

In this section, we will discuss about the electronic structure of the proton transfer group and dielectric environment effect for the proton transfer machinery.

3.2.1 Electron density map

We support our argument that donor-accepter getting closer will help lower the energy barrier by using the electron density map, which is shown in Figure 3.11. In Figure 3.11, the red color represents the highest density, which corresponds to core electrons that achieved their maximum density around each atom. The other colors, following the order of Yellow, Green, to Blue represent less dense of electron cloud. The color scale is also shown in the Figure 3.11.

From the comparison of electron density maps for these different donor-accepter distances, we find that the electron density changed in the region between donor and acceptor. When donor-accepter distance is 2.80\AA , this region shows no color, which means there is no apparent distribution of electron cloud. But when donor-accepter distance is 2.49\AA , this region shows green color, which means higher electron density distribution in this region. Because when densities from two different molecules are similar (meaning change of electron cloud is limited) then the proton is easier to pass, which means the barrier is lower.

Due to the change in the electron density, the energy barrier is lowered after bringing the donor and the acceptor closer. The way that hydrogen bond bridge changes the barrier is to increase the electron density between the donor and the acceptor. And the way hydrogen bond switch changes the energy landscape is first decrease the energy minimum in the acceptor side and then increase the energy minimum in the donor side. **(Conclusion 2)**

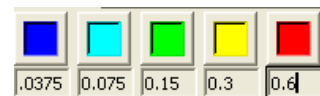
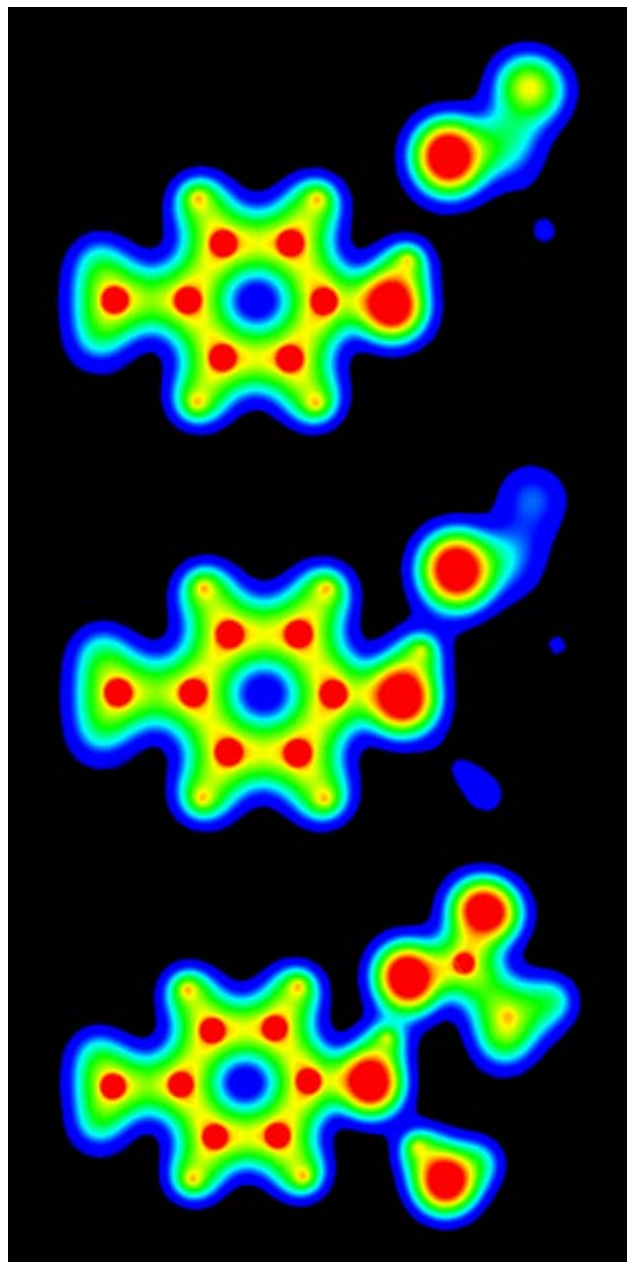


Figure 3.11 Electron density map of three structural elements in proton transfer. Upper: DA=2.80Å, Middle: DA=2.60Å and bottom DA=2.49Å. The color scheme is shown in the right. Unit is Coulomb/Bohr³

3.2.2 Dielectric environment

The calculation results we present now are performed in vacuum ($\epsilon=1$). The reason and procedure of how we perform the dielectric constant calculation is described in chapter II.

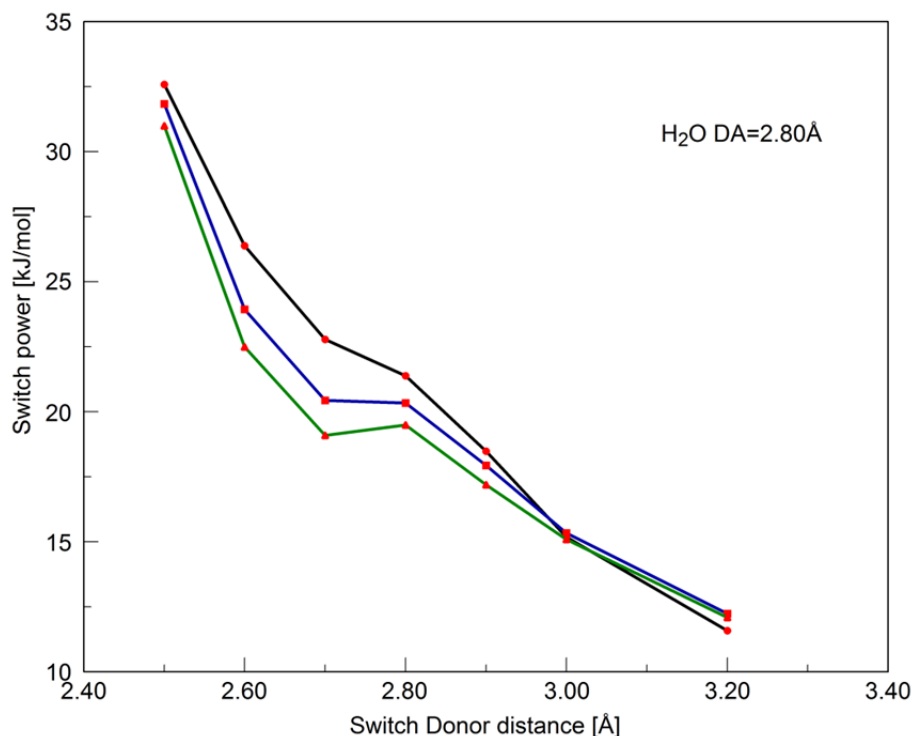


Figure 3.12 Switch power of different proton transfer switch-donor distance in different dielectric environment of 2.02(Black), 4.33(Blue), 6.89(Green) and H₂O is the hydrogen bond switch.

Figure 3.12 gave the results of calculations with consideration of dielectric environment. We find that for the same switch-donor distance, calculations with 2.02 (dielectric environment) have higher switch power compared to that of 4.33(dielectric environment) and 6.89(dielectric environment). In addition, if we compare the difference between 2.02 and 4.33 and the difference between 4.33 and 6.89, then we find that the latter has less a difference. **From these, we could conclude that the dielectric environment will reduce the switch power but the effect on reducing is less as dielectric constant goes to higher value.(Conclusion 3)** This implies as dielectric constant becomes higher, there is a lower limit of switch power that hydrogen bond

switch could provide. This means hydrogen bond switch is still able to trigger the proton transfer inside protein with consideration of dielectric constant.

REFERENCE

1. Xie, A., et al., *Formation of a new buried charge drives a large-amplitude protein quake in photoreceptor activation*. *Biochemistry*, 2001. 40(6): p. 1510-1517.
2. Hoff, W., *Photoactive Yellow Protein. A New family of Eubacterial Blue-Light Photoreceptors*, 1995, University of Amsterdam.
3. Klaas, J.H., H. Johnny, and G. Thomas, *Photoactive Yellow Protein, A New Type of Photoreceptor Protein: Will This "Yellow Lab" Bring Us Where We Want to Go? //*. *The Journal of Physical Chemistry A*, 2003. 107.
4. Marx, D., *Proton transfer 200 years after von Grothuss: insights from ab initio simulations*. *Chemphyschem : a European journal of chemical physics and physical chemistry*, 2006. 7(9): p. 1848-1870.
5. Cao, Y., et al., *Proton transfer from Asp-96 to the bacteriorhodopsin Schiff base is caused by a decrease of the pKa of Asp-96 which follows a protein backbone conformational change*. *Biochemistry*, 1993. 32(8): p. 1981-1990.
6. Xie, A., et al., *Glu46 donates a proton to the 4-hydroxycinnamate anion chromophore during the photocycle of photoactive yellow protein*. *Biochemistry*, 1996. 35(47): p. 14671-14678.
7. Lanyi, J., *Proton transfers in the bacteriorhodopsin photocycle*. *Biochimica et biophysica acta*, 2006. 1757(8): p. 1012-1018.
8. Jeffrey, G.A., *An introduction to hydrogen bonding*. 1997: Oxford University Press.
9. Steve, S., *Hydrogen bonding: a theoretical perspective*, 1997, Oxford University Press: New York.
10. Emsley, J., *Very strong hydrogen bonding*. *Chemical Society Reviews*, 1980. 9(1): p. 91-124.
11. Murthy, A.S.N. and C.N.R. Rao, *Spectroscopic Studies of the Hydrogen Bond*. *Applied Spectroscopy Reviews*, 1968. 2(1): p. 69-191.
12. Hobza, P. and Z. Havlas, *Blue-Shifting Hydrogen Bonds*. *Chemical reviews*, 2000. 100(11): p. 4253-4264.
13. Glushkov, V.N. and S. Wilson, *On the Coulson-Fischer wave function and a local static correlation potential*. *Molecular Physics*, 2011. 110(3): p. 149-161.
14. Singh, U. and P.A. Kollman, *A water dimer potential based on ab initio calculations using Morokuma component analyses*. *The Journal of chemical physics*, 1985. 83: p. 4033.
15. Pauling, L., R.B. Corey, and H.R. Branson, *The structure of proteins: Two hydrogen-bonded helical configurations of the polypeptide chain*. *Proceedings of the National Academy of Sciences*, 1951. 37.
16. Pauling, L. and R. Corey, *Configurations of Polypeptide Chains With Favored Orientations Around Single Bonds: Two New Pleated Sheets*. *Proceedings of the*

- National Academy of Sciences of the United States of America, 1951. 37(11): p. 729-740.
17. Tapas, K. and S. Steve, *Cooperativity of conventional and unconventional hydrogen bonds involving imidazole*. International Journal of Quantum Chemistry, 2006. 106.
 18. Wieczorek, R. and J. Dannenberg, *Hydrogen-bond cooperativity, vibrational coupling, and dependence of helix stability on changes in amino acid sequence in small 3 10-helical peptides. A density functional theory study*. Journal of the American Chemical Society, 2003. 125(46): p. 14065-14071.
 19. Voet, D.V., J., *Biochemistry*. 3 ed. 2004: John Wiley & Sons, Inc.
 20. Devanathan, S., et al., *Early photocycle kinetic behavior of the E46A and Y42F mutants of photoactive yellow protein: femtosecond spectroscopy*. Biophysical journal, 2001. 81(4): p. 2314-2319.
 21. Otto, H., et al., *Substitution of amino acids Asp-85, Asp-212, and Arg-82 in bacteriorhodopsin affects the proton release phase of the pump and the pK of the Schiff base*. Proceedings of the National Academy of Sciences of the United States of America, 1990. 87(3): p. 1018-1022.
 22. Mogi, T., et al., *Aspartic acid substitutions affect proton translocation by bacteriorhodopsin*. Proceedings of the National Academy of Sciences of the United States of America, 1988. 85(12): p. 4148-4152.
 23. Genick, U., et al., *Active site mutants implicate key residues for control of color and light cycle kinetics of photoactive yellow protein*. Biochemistry, 1997. 36(1): p. 8-14.
 24. Devanathan, S., et al., *Dual photoactive species in Glu46Asp and Glu46Ala mutants of photoactive yellow protein: a pH-driven color transition*. Biochemistry, 1999. 38(41): p. 13766-13772.
 25. Mihara, K., et al., *Functional expression and site-directed mutagenesis of photoactive yellow protein*. Journal of biochemistry, 1997. 121(5): p. 876-880.
 26. Meyer, T., *Isolation and characterization of soluble cytochromes, ferredoxins and other chromophoric proteins from the halophilic phototrophic bacterium Ectothiorhodospira halophila*. Biochimica et biophysica acta, 1985. 806(1): p. 175-183.
 27. Sprenger, W., et al., *The eubacterium Ectothiorhodospira halophila is negatively phototactic, with a wavelength dependence that fits the absorption spectrum of the photoactive yellow protein*. Journal of bacteriology, 1993. 175(10): p. 3096-3104.
 28. Hoff, W., et al., *Thiol ester-linked p-coumaric acid as a new photoactive prosthetic group in a protein with rhodopsin-like photochemistry*. Biochemistry, 1994. 33(47): p. 13959-13962.
 29. Nie, B., J. Stutzman, and A. Xie, *A vibrational spectral marker for probing the hydrogen-bonding status of protonated Asp and Glu residues*. Biophysical journal, 2005. 88(4): p. 2833-2847.
 30. Koradi, R., M. Billeter, and K. Wüthrich, *MOLMOL: A program for display and analysis of macromolecular structures*. Journal of Molecular Graphics, 1996. 14(1): p. 51-55.
 31. System, T.P.M.G., *Version 1.2r3pre*. Schrödinger, LLC.

32. Nagle, J.F. and H.J. Morowitz, *MOLECULAR MECHANISMS FOR PROTON TRANSPORT IN MEMBRANES*. Proceedings of the National Academy of Sciences of the United States of America, 1978. 75(1): p. 298-302.
33. Patrick, G., *100 years of the hydrogen bond*. Nature Chemistry, 2012. 4(11): p. 863-864.
34. Hohenberg, P. and W. Kohn, *Inhomogeneous electron gas*. Physical Review, 1964. 136(3B).
35. Kohn, W. and L.J. Sham, *Self-Consistent Equations Including Exchange and Correlation Effects*. Physical Review, 1965. 140(4A): p. A1133-A1138.
36. Skylaris, C.-K., et al., *Introducing [small-caps ONETEP]: Linear-scaling density functional simulations on parallel computers*. The Journal of Chemical Physics, 2005. 122(8): p. 084119-10.
37. Springborg, M., *Methods of electronic-structure calculations*. Wiley Chichester, 2000.
38. Bachman, G., *Functional Analysis*. 1998: Dover.
39. Kohn, W., *Nobel Lecture: Electronic structure of matter—wave functions and density functionals*. Reviews of Modern Physics, 1999. 71(5): p. 1253-1266.
40. Becke, A.D., *Density functional thermochemistry. III. The role of exact exchange*. The Journal of Chemical Physics, 1993. 98: p. 5648.
41. Lars, G. and G. Stefan, *Efficient and Accurate Double-Hybrid-Meta-GGA Density Functionals—Evaluation with the Extended GMTKN30 Database for General Main Group Thermochemistry, Kinetics, and Noncovalent Interactions*. Journal of Chemical Theory and Computation, 2011. 7.
42. Perdew, J.P., et al., *Atoms, molecules, solids, and surfaces: Applications of the generalized gradient approximation for exchange and correlation*. Physical Review B, 1992. 46(11): p. 6671-6687.
43. Perdew, J.P., K. Burke, and M. Ernzerhof, *Generalized Gradient Approximation Made Simple*. Physical Review Letters, 1996. 77(18): p. 3865-3868.
44. Becke, A.D., *Density-functional exchange-energy approximation with correct asymptotic behavior*. Physical Review A, 1988. 38(6): p. 3098-3100.
45. Lee, Yang, and Parr, *Development of the Colle-Salvetti correlation-energy formula into a functional of the electron density*. Physical review. B, Condensed matter, 1988. 37(2): p. 785-789.
46. Tao, J., et al., *Climbing the Density Functional Ladder: Nonempirical Meta-Generalized Gradient Approximation Designed for Molecules and Solids*. Physical Review Letters, 2003. 91(14): p. 146401.
47. Vosko, S.H., L. Wilk, and M. Nusair, *Accurate spin-dependent electron liquid correlation energies for local spin density calculations: a critical analysis*. Canadian Journal of Physics, 1980. 58(8): p. 1200-1211.
48. Stephens, P.J., et al., *Ab Initio Calculation of Vibrational Absorption and Circular Dichroism Spectra Using Density Functional Force Fields*. The Journal of Physical Chemistry, 1994. 98.
49. Zhao, Y. and D.G. Truhlar, *Hybrid Meta Density Functional Theory Methods for Thermochemistry, Thermochemical Kinetics, and Noncovalent Interactions: The MPW1B95 and MPWB1K Models and Comparative Assessments for*

- Hydrogen Bonding and van der Waals Interactions*. The Journal of Physical Chemistry A, 2004. 108(33): p. 6908-6918.
50. Boys, S.F., Proc. Roy. Soc. Ser A, 1950. 200.
 51. Ernest, R.D. and F. David, *Basis set selection for molecular calculations*. Chemical Reviews, 1986. 86.
 52. McMurchie, L.E. and R.D. Ernest, *One- and Two- Electron Integrals over Cartesian Gaussian Functions*. Journal of Computational Physics, 1978. 26(2): p. 218.
 53. Foresman, J.B.F.E., *Exploring chemistry with electronic structure methods*. 1996, Pittsburgh, Pa.: Gaussian.
 54. Daza, M.C., et al., *Basis set superposition error-counterpoise corrected potential energy surfaces. Application to hydrogen peroxide X (X= F, Cl, Br, Li, Na) complexes*. The Journal of chemical physics, 1999. 110: p. 11806.
 55. Boys, S.F. and F. Bernardi, *The calculation of small molecular interactions by the differences of separate total energies. Some procedures with reduced errors*. Molecular Physics, 1970. 19(4): p. 553-566.
 56. Vyacheslav, S.B., et al., *Evaluation of B3LYP, X3LYP, and M06-Class Density Functionals for Predicting the Binding Energies of Neutral, Protonated, and Deprotonated Water Clusters*. Journal of Chemical Theory and Computation, 2009. 5.
 57. Lozynski, M., D. Rusinska-Roszak, and H.-G. Mack, *Hydrogen Bonding and Density Functional Calculations: The B3LYP Approach as the Shortest Way to MP2 Results*. The Journal of Physical Chemistry A, 1998. 102(17): p. 2899-2903.
 58. Tushar van der, W., et al., *Performance of various density functionals for the hydrogen bonds in DNA base pairs*. Chemical Physics Letters, 2006. 426.
 59. Mariam, Y.H. and R.N. Musin, *A B3LYP study of intramolecular hydrogen bonding and proton transfer in naphthazarin: a model system for daunomycin/adriamycin*. Journal of Molecular Structure: THEOCHEM, 2001. 549(1-2): p. 123-136.
 60. Prabhat, K.S., C. Ajay, and L. Shyi-Long, *Theoretical investigation for the hydrogen bond interaction in THF-water complex*. Chemical Physics Letters, 2004. 386.
 61. M. J. Frisch, G.W.T., H. B. Schlegel, G. E. Scuseria, M. A. Robb, J. R. Cheeseman, J. A. Montgomery, Jr., T. Vreven, K. N. Kudin, J. C. Burant, J. M. Millam, S. S. Iyengar, J. Tomasi, V. Barone, B. Mennucci, M. Cossi, G. Scalmani, N. Rega, G. A. Petersson, H. Nakatsuji, M. Hada, M. Ehara, K. Toyota, R. Fukuda, J. Hasegawa, M. Ishida, T. Nakajima, Y. Honda, O. Kitao, H. Nakai, M. Klene, X. Li, J. E. Knox, H. P. Hratchian, J. B. Cross, V. Bakken, C. Adamo, J. Jaramillo, R. Gomperts, R. E. Stratmann, O. Yazyev, A. J. Austin, R. Cammi, C. Pomelli, J. W. Ochterski, P. Y. Ayala, K. Morokuma, G. A. Voth, P. Salvador, J. J. Dannenberg, V. G. Zakrzewski, S. Dapprich, A. D. Daniels, M. C. Strain, O. Farkas, D. K. Malick, A. D. Rabuck, K. Raghavachari, J. B. Foresman, J. V. Ortiz, Q. Cui, A. G. Baboul, S. Clifford, J. Cioslowski, B. B. Stefanov, G. Liu, A. Liashenko, P. Piskorz, I. Komaromi, R. L. Martin, D. J. Fox, T. Keith, M. A. Al-Laham, C. Y. Peng, A. Nanayakkara,

- M. Challacombe, P. M. W. Gill, B. Johnson, W. Chen, M. W. Wong, C. Gonzalez, and J. A. Pople, Gaussian, Inc., *Gaussian 03, Revision C.02*. Wallingford CT, 2004.
62. Schutz, C.N. and A. Warshel, *What are the dielectric "constants" of proteins and how to validate electrostatic models?* *Proteins: Structure, Function, and Bioinformatics*, 2001. 44(4): p. 400-417.
 63. Li, L., et al., *On the Dielectric "Constant" of Proteins: Smooth Dielectric Function for Macromolecular Modeling and Its Implementation in DelPhi*. *J Chem Theory Comput*, 2013. 9(4): p. 2126-2136.
 64. Miertuš, S., E. Scrocco, and J. Tomasi, *Electrostatic interaction of a solute with a continuum. A direct utilization of AB initio molecular potentials for the prevision of solvent effects*. *Chemical Physics*, 1981. 55.
 65. Miertuš, S. and J. Tomasi, *Approximate evaluations of the electrostatic free energy and internal energy changes in solution processes*. *Chemical Physics*, 1982. 65.
 66. Morse, P.M., *Diatomic molecules according to the wave mechanics. II. vibrational levels*. *Physical Review*, 1929. 34(1): p. 57.
 67. L D Landau, E.M.L., *Quantum Mechanics:Non-Relativistic Theory*. 1981: Elsevier Ltd.
 68. Walter, R.P.S., et al., *The GROMOS Biomolecular Simulation Program Package*. *The Journal of Physical Chemistry A*, 1999. 103.
 69. Bernard, R.B., et al., *CHARMM: A program for macromolecular energy, minimization, and dynamics calculations*. *Journal of Computational Chemistry*, 1983. 4.
 70. Henderson, J.N., et al., *Excited State Proton Transfer in the Red Fluorescent Protein mKeima*. *Journal of the American Chemical Society*, 2009. 131(37): p. 13212-13213.

Appendix A Gaussian03 Commands

Jun 3, 2011

Part A. Geometry Optimization

- **Create the initial geometry as best as you can, including bond length, bond angle, dihedral angle, and hydrogen bond interactions. (This step is very critical.)**

N1 N2 (below geometry data with one empty line, and followed with one empty line)
(N1 is the hydrogen bond donor, while N2 is the hydrogen bond acceptor)

- **Choose the memory and check point file:**

```
%MEM=1GB  
%chk=Asp_water=2_pH=12_HPC_0306_2011_SD.chk
```

- **Choose the hard drive capacity (for MPn and CCSD(T) calculation):**

```
#CCSD=(T)/6-311+G(2df,pd) opt=( z-matrix) MaxDisk=10GB scf=direct Freq test
```

- **Optimize the initial geometry using PM3 (empirical method)**

```
#PM3 scf=direct Opt=(z-matrix,maxcyc=512) Test
```

- **Calculate energy using z-matrix (internal coordinates), use this command**

```
#B3LYP/6-311G(d) scf=Direct Opt=(z-matrix, maxcyc=512) Test
```

D

i

You may use different QM methods: examples HF, B3LYP,MP2

Different basis sets: 6-31G(d), 6-311+G(2d,p),6-311+G(2df,pd) (may add to this

list)

- **Calculate energy using Cartesian coordinates, use this command (Proton transfer uses this coordinate.)**

```
#B3LYP/6-311G(d) SCF=Direct Opt=ModRedun Test
```

- **For Continuation of calculation, use this command**

Continue to calculate energy using more accurate method

```
--Link1--  
%MEM=1GB  
%chk=Asp_water=2_pH=12_HPC_0306_2011_SD  
#B3LYP/6-311+G(2d,p) Geom=Allcheck scf=direct Test
```

Continue to calculate frequency using optimized structure (saved in checkpoint file)

```
--Link1--  
%MEM=1GB  
%chk=Asp_water=2_pH=12_HPC_0306_2011_SD  
#B3LYP/6-31G(d) Geom=Allcheck scf=direct Freq Test
```

Continue to calculate the isotope effect (suppose (DOD...OD))

```
--Link1--  
%chk=H2O_OH(-)_HB_B3LYP_6-311_SD_May2011  
%Mem=1000MB  
#B3LYP/6-311+G(2d,p) Geom=Allcheck scf=direct Freq(ReadFC,ReadIsotope)  
Test  
  
300 1  
16  
2  
2  
16  
2
```

Continue to calculate energy with optimized structure (saved in checkpoint file) in other solvent

```
%chk=Tyr[0]_COO[-]_B_OH=111_HPC_04082011_SD  
%MEM=2000MB  
#B3LYP/6-311+G(2d,p) Geom=AllCheck SCRF=(PCM,Solvent = CycloHexane,  
read) Test
```

```
SPHEREONH=12
```

```
--Link1--
```

```
%chk=Tyr[0]_COO[-]_B_OH=111_HPC_04082011_SD
%MEM=2000MB
#B3LYP/6-311+G(2d,p) Geom=AllCheck SCRF=(PCM,Solvent=Ether,read) Test
SPHEREONH=12
```

--Link1--

```
%chk=Tyr[0]_COO[-]_B_OH=111_HPC_04082011_SD
%MEM=2000MB
#B3LYP/6-311+G(2d,p) Geom=AllCheck SCRF=(PCM,Solvent=Aniline,read)
```

Test

```
SPHEREONH=12
```

SPHEREONE= N; here N is the boundary of electron potential; In proton transfer calculation, this is the number of hydrogen that moves within O...O bond.

Part B Energy Calculation

1. Structure Optimization:

```
#PM3 scf=direct Opt=(loose,z-matrix)
```

2. For general calculation in vacuum:

```
#B3LYP/6-311+G(2d,p) scf=direct Opt=(loose,z-matrix)
```

3. For general calculation in solvent:

```
#B3LYP/6-311+G(2d,p) SCRF=(PCM,Solvent=DMSO)
```

4. For general calculation in solvent :(put a sphere on H No.15)

```
#B3LYP/6-311+G(2d,p) SCRF=(PCM,Solvent=DMSO,read)
```

```
SPHEREONH=15
```

Part C. Frequency Calculation:

For general calculation in vacuum:

#B3LYP/6-311+G(2d,p) scf=direct Opt=Modredun Freq

-----Additional Step-----

#B3LYP/6-311+G(2d,p) Geom=Allcheck scf=direct Opt=Modredun Freq

Isotopic Labeling

#B3LYP/6-311+G(2d,p) scf=direct Geom=AllCheck

Freq(ReadFC,ReadIsoltops)Test

Last command should together with a changed mass of isotope atom in atom list.

Part D. Convergent requirements:

(Opt=loose)

Max Force: 0.002500
RMS Force: 0.001667
Max Displacement: 0.010000
RMS Displacement: 0.006667

(Opt=Normal)

Max Force: 0.000450
RMS Force: 0.000300
Max Displacement: 0.001800
RMS Displacement: 0.001200

Appendix B: Electron Density Map

I. Introduction

After a long calculation using quantum chemistry, we need a way to extract meaningful data to analyze and present as enlightening as possible. Such techniques like NBO (Natural Bond Orbital) analysis, HUMO/LUMO electron density distribution, molecular orbital, electron momentum distribution, etc. Here we introduce a kind of map that is suitable to analyze weak interactions—electron density difference map.

Three things to reduce artifacts are:

- a. The position of interest atoms must be precisely fixed because the density difference is very sensitive.
- b. The two files to make difference map must have same grid.
- c. Although we didn't use here, but the BSSE (basis sets superposition error) correction is recommended for quantitative analysis of electron density difference map.

In the steps described in part II, following software are required:

- a. Gaussian 03 (G03) & Gaussian View and its utility programs: formchk.exe, cubegen.exe, cubman.exe
- b. UCSF Chimera.

II. How to plot

Major steps are:

- a. **Extract electron density data and compute their difference value on given grids;**
- b. **Plot graph of the given electron density difference data.**

Detail steps:

a1. Fix O...O...C atoms in one plane in a previous input. Use GV to open the desired input file. In View=>z-matrix editor, find the two O atoms between which the proton is moving. Manually number these two atoms O1 and O2 (Fig.1) and save the input in Cartesian coordinate format. Now the atom O1 and O2 is fixed in one line. Then number the C atom the 3rd atom. Now the O...O...C are in xoz plane.

In z-matrix (internal coordinate system), the 1st atom is defined as origin and the 1st-2nd atom define the x-z axis, then the 3rd is perpendicular xoz plane.

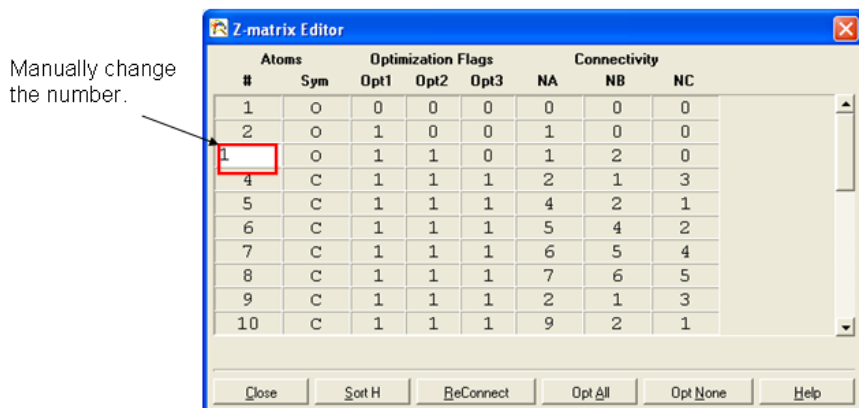


Fig.1 Manually change the atom number and save as input file in GV.

a2. Change O...O...C from xoz plane to xoy plane. Use Excel to open the input file: Choose delimited → check “space”. Then interchange the data in 2nd column with 3rd column. By doing this the y and z coordinates are inter-changed.(Fig.2) Save file and open it using “notepad.exe” to check if the spaces/separators are correct.

Tips: In GV, the screen is xoz plane while in Chimera and other more commonly seen software, the screen is xoy plane.

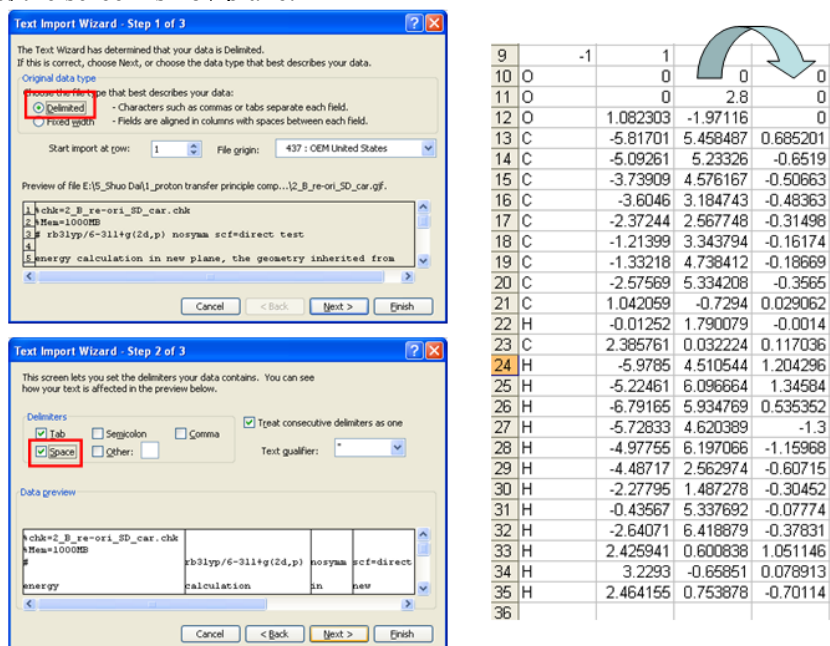


Fig.2. Use Excel to open and interchange the y and z coordinates.

a3. Redo the calculation using new inputs and save the check point file. Since we have a previous optimized structure, so what we need is only to calculate the energy so that the check point file can have corresponding electron density data. If this is a new calculation, we need opt as well.

For a previous optimized structure:

```
#B3LYP/6-311+(2d,p) scf=direct nosymm test
```

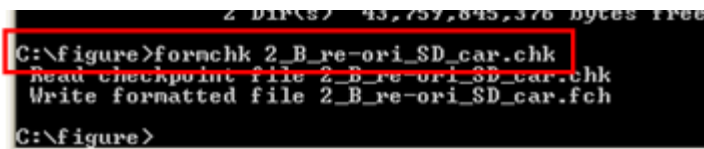
For a new calculation:

```
#B3LYP/6-311+(2d,p) scf=direct opt=(loose) nosymm test
```

The keyword “nosymm” is to force G03 to use current coordinates without changing it to a more symmetrical position which is ideal for the purpose of calculation.

a4. Unformat the check point file using G03 utility program. From a G03 check point file, we use G03 utility program “formchk.exe” to decode this binary file (formatted file) into text format file (unformatted file)(Fig.3). If the check point file is from HPC calculation, you should perform this step on HPC and then it will become text format file.

Tips: If you want, you can run G03 utility program “unfchk.exe” on PC to turn this text format file back into binary file, which then can be used by G03 PC version. This serves a way to convert check point file between different platforms.



```
C:\figure>formchk 2_B_re-ori_SD_car.chk
Read checkpoint file 2_B_re-ori_SD_car.chk
Write formatted file 2_B_re-ori_SD_car.fch
C:\figure>
```

Fig.3 Use G03 utility program formchk.exe to convert *.chk to *.fch.

a5. Use G03 utility “cubegen.exe” program to compute the value on given grids for the first file. Run “cubegen.exe” to read the first *.fchk file and use the parameters as Fig.4 shows. Then use notepad.exe or any text editors to open *.cube file and record the first value in the position as shown in Fig.5.

The numbers recorded in *.cube file are in atomic unit, which means the length unit is Bohr and the density unit is Column/Bohr³. The parameters input represent:

- 1: Grid number will be given manually below
- 2: Use 3 points/Bohr
- 3: Use 6 points/Bohr
- 4: Use 12 points/Bohr
- 0: Always use 80³ points for the whole system.

parameters recorded from the first file. Note when inputting the data, use “-” to indicate this number is in Bohr unit, which is shown in Fig.6.

a7. Use G03 utility “cubman.exe” program to compute the difference of the two files. The corresponding input is shown in fig.7. Note, we will use acceptor state minus donor state.

```

C:\WINDOWS\system32\cmd.exe
Header in cube file [H]? h
^C
C:\figure>cubman
Action [Add, Copy, Difference, Properties, Subtract, Scale, Square]? SU
First input? 2_D_re-ori_SD_car.cube
Is it formatted [no,yes,old]? y
Opened special file 2_D_re-ori_SD_car.cube.
Second input? 2_B_re-ori_SD_car.cube
Is it formatted [no,yes,old]? y
Opened special file 2_B_re-ori_SD_car.cube.
Output file? diff_D-B.cube
Should it be formatted [no,yes,old]? y
Opened special file diff_D-B.cube.
Input file titles:
energy calculation in new plane, the geometry inherited from Tyr(0)_C00< densit
Electron density from Total SCF Density
Input file titles:
energy calculation in new plane, the geometry inherited from Tyr(0)_C00< densit
Electron density from Total SCF Density
SumAP= 71.9466672099 SumAN= -0.0000883288 SumA= 71.9465788812
CAMax= 2.3643100000 XYZ= 2.9606880000 -3.0106880000 -0.0699090000
CAMin= -0.0000018754 XYZ= 4.0976880000 14.0443120000 2.2040910000
SumBP= 71.9569186640 SumBN= -0.0001349819 SumB= 71.9567836821
CBMax= 1.8225800000 CBMin= -0.0000029542
SumOP= 27.0421814885 SumON= -27.0523862895 SumO= -0.0102048010
COMax= 2.0806020000 COMin= -1.7209080000
DipAE= 209.4732876778 -364.9873594527 -34.2910690108
DipAN= -286.0054150000 496.5572040000 45.2693250000
DipA= -76.5321273222 131.5698445473 10.9782559892
DipBE= 214.2244258555 -351.1210201362 14.4784939094
DipBN= -294.2220980000 481.3531940000 -21.3520650000
DipB= -79.9976721445 130.2321738638 -6.8735710906
DipOE= -4.7511381778 -13.8663393165 -48.7695629201
DipON= -286.0054150000 496.5572040000 45.2693250000
DipO= -290.7565531778 482.6908646835 -3.5002379201
C:\figure>

```

Fig.7 Use G03 utility “cubman.exe” program to compute the difference of the two files. We use acceptor minus donor state.

b1. Start UCSF Chimera and open the difference *.cube file and plot the 3D map. Since the molecule is placed in the xoy plane, so the position of the molecule when file is open, is already in the xoy plane.

When you open the *.cube file, the “Volume Viewer” will pop automatically. You can set the cut-off value here. In its menu “Tools” → surface color. **Choose by “volume data value”**. Then input the color scheme and press enter to let it come into effect. (Fig.8 & Fig.9)

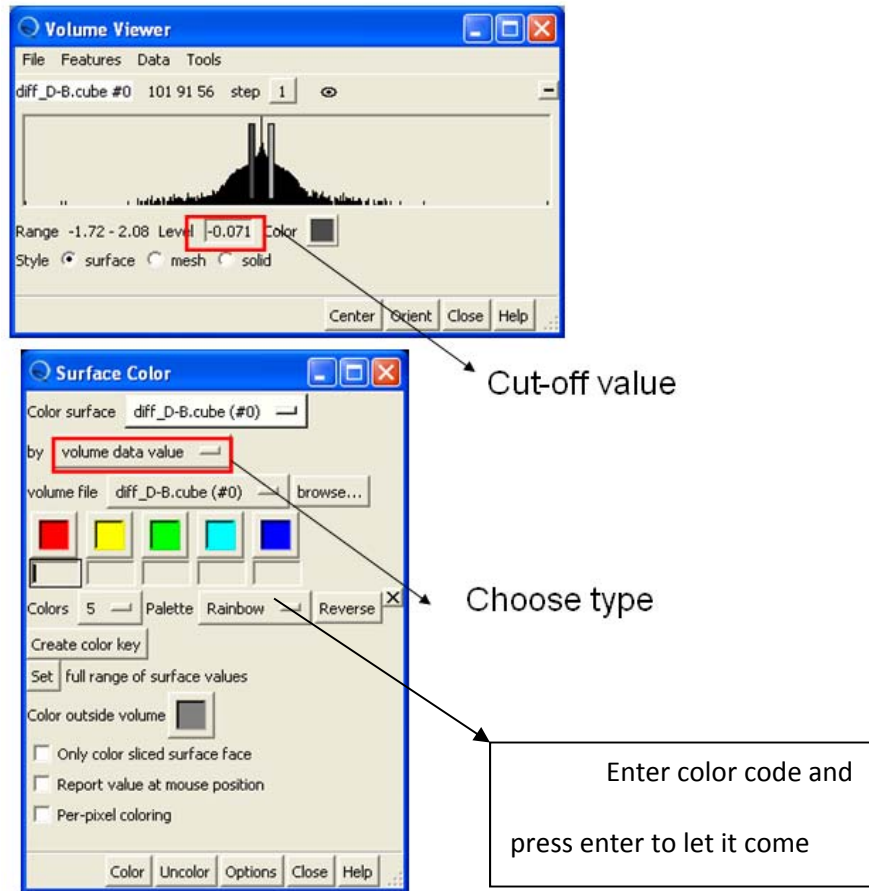


Fig.8 how to load and display the data with color.



Fig.9 color schemes suggested for Glu+Tyr system. Left two are for difference density map, right most is for normal density map.

b2. Use a plane to see the middle 2D map. In the UCSF Chimera main window (not Volume Viewer window), we choose Tools → Viewing control → Side view. In the Camera Tab, since the O...O...C are in the xoy plane, we set near plane to “0” position, which will cut the

system right in the middle. In the Side View Tab, press surface capping button and set the Mesh subdivision factor to be 6. (Fig.10)

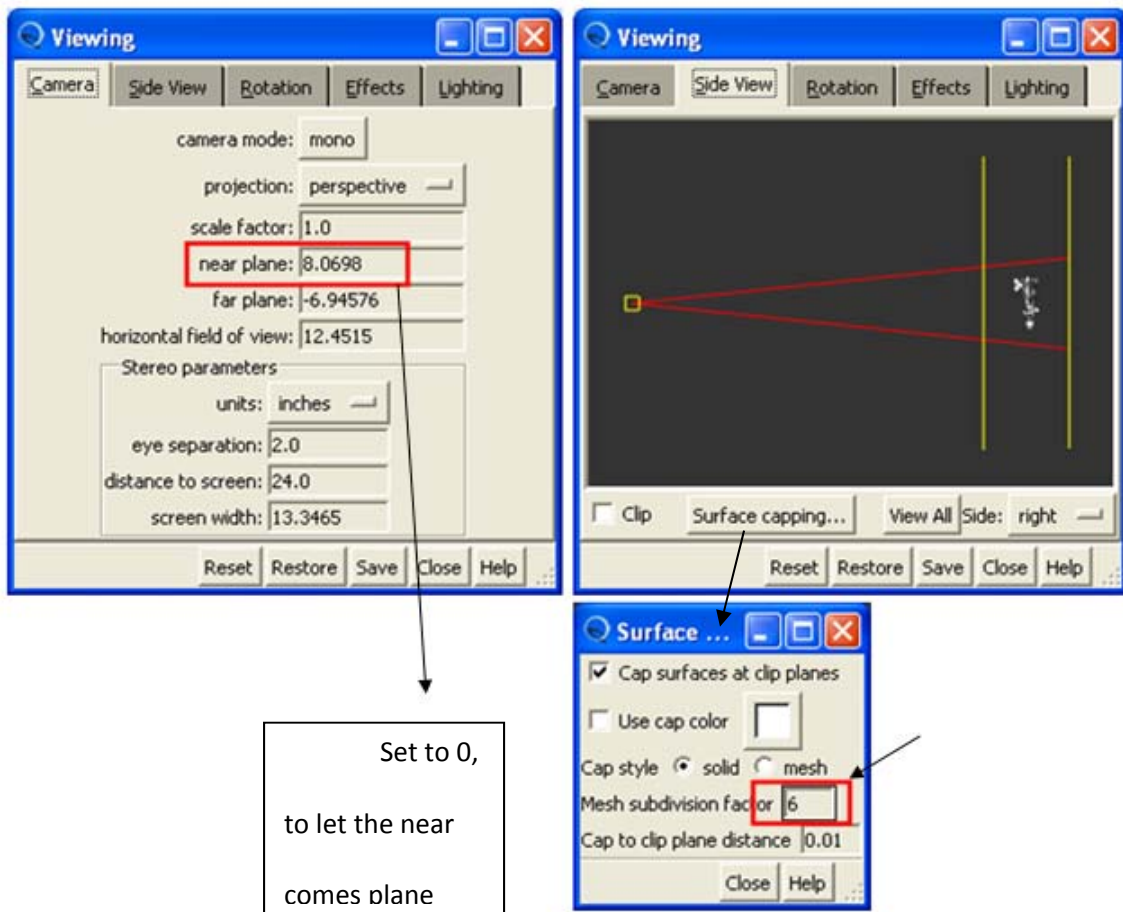
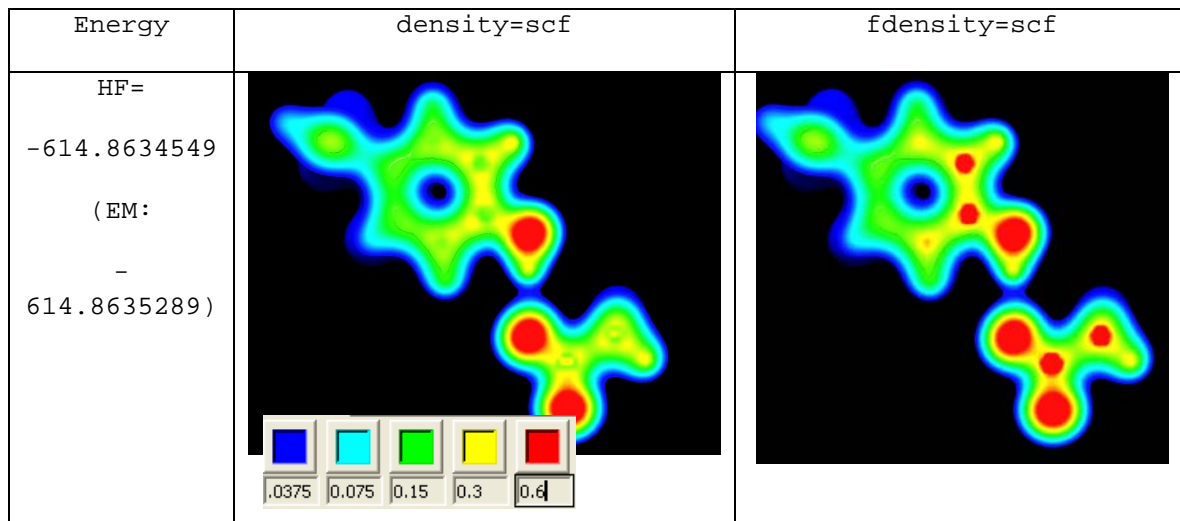


Fig.10 Side-View 2D map.

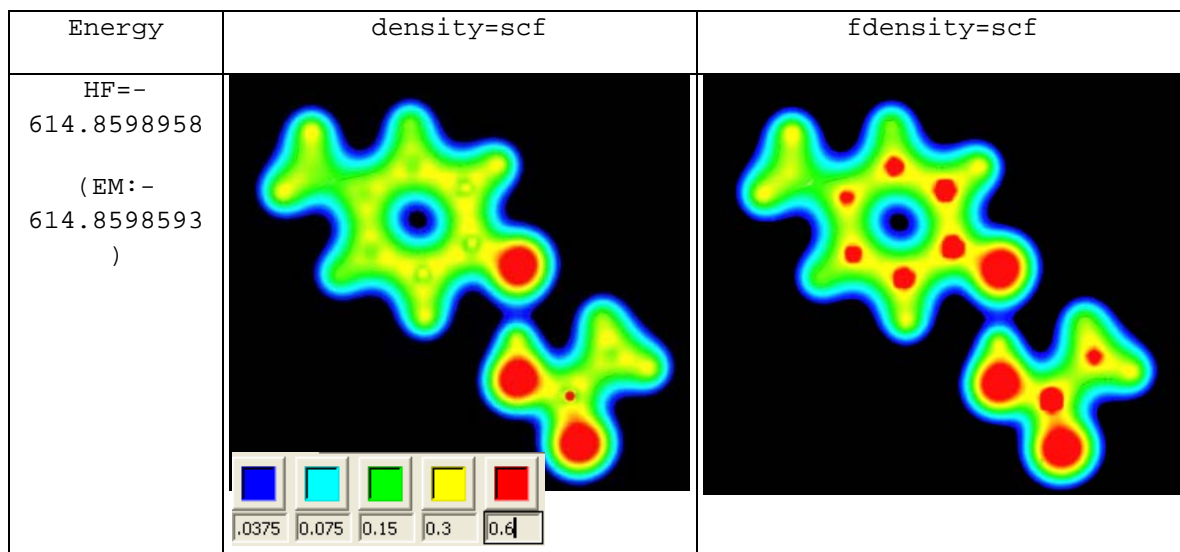
b3. Output the structure into TIF image. File→save image→give a filename to *.tif file and press “Save as”.

III. Results

1. The density map of state B of Phase III:

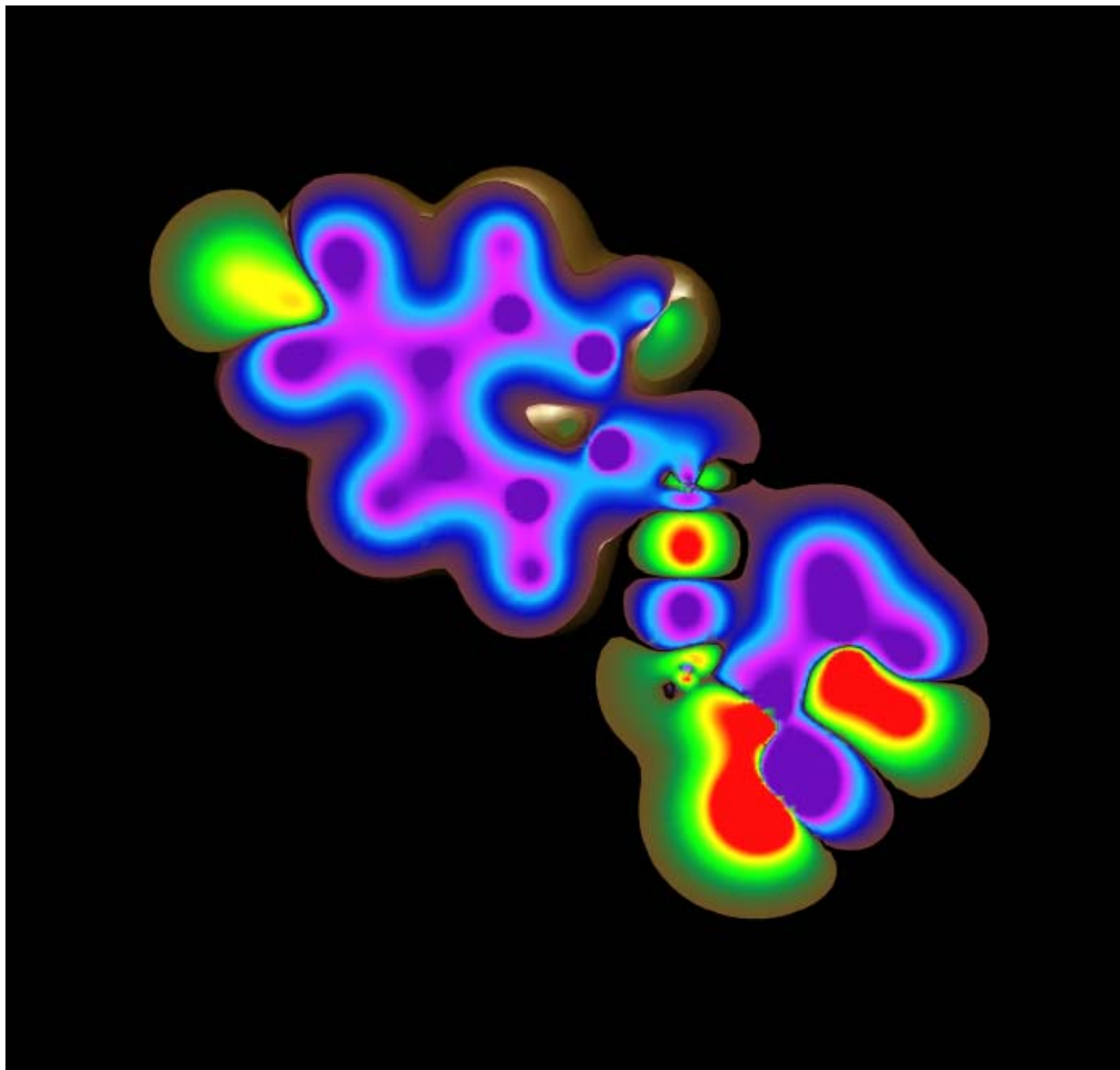


2. The density map of state D of Phase III:



Color scheme used for next page graph:





Electron Density Distribution for Proton Transfer

Shuo Dai

Oklahoma State University

Appendix C Partial List of Proteins with Proton Transfer

LRPT: Long range proton transport (translocation); ESPT: excite state

proton transfer; PCET: proton coupled electron transfer

Protein Name(Family)	Biological function	Description (Donor, Acceptor etc.)
Bio-energetic:7		
Bacteriorhodopsin	Light-driven proton pump (<i>Halobacterium halobium</i>)	Direction: Schiff base → Asp85(L ₅₅₀ → M _{410(EC)}) Asp96 → Schiff base(M _{410(EC)} → N ₅₆₀) Asp85 → Proton release group (Glu204, Glu194?) (O ₆₄₀ → bR ₅₄₀) Event happened per cycle: 3 Type: LRPT(Long range proton transport)
Cytochrome c oxidase (Heme-copper oxidase)	Redox-driven proton pump (Bateria)	Direction: Event happened per cycle: several Type: PCET(proton coupled electron transfer) & LRPT
Ferredoxin I (Iron-sulfur Protein)	Redox-driven proton pump (Bateria)	Direction: Event happened per cycle: several Type: PCET & LRPT
Photosynthetic Reaction Center	Convert light energy to chemical energy and electro-chemical potential	Direction: His-L126 → Asp-L210 Asp-L210 → Asp-L213 Asp-L213 → Glu-L212 Glu-L212 → Q _B His-L126 → Asp-L210 Asp-L210 → Asp-L213 Asp-L213 → Ser-L223 Ser-L223 → Q _B Event happened per cycle: 6 Type: LRPT
Arsenite oxidase		Type: PCET
ATPase	Convert electro-chemical potential to chemical bond energy	Type: PCET
Xanthorhodopsin	Convert light energy to chemical energy and electro-chemical potential	Type: ESPT(excite state proton transfer)
Signaling: 4		
PYP(PAS domain)	signaling	Direction: Glu46 → pCA Event happened per cycle: 1 Type: basic PT
GFP	signaling	Direction:

		Event happened per cycle: Type: ESPT
TePixD (BluF domain)	Signaling	
Sensory Rhodopsin I	Signaling	Type: LRPT
Rhodopsin	Signaling	Type:LRPT
mKeima	Signaling[70]	Intro: Tetramer(each 25kD), excited in blue and emitted red color. Direction: from Chromophore hydroxyl via Ser142 to Asp 157 Type: ESPT; 3IR8
Catalysis(Enzyme): 20		
Protease		
Serine protease (e.g. trypsin)	Active site using serine; relate to human Batten disease	Peptidases or proteinases are now classified into 7 families based on the nature of the catalytic residues. They are aspartic-(first described in1993), cysteine-(1993), serine-(1993) metallo-(1993), threonine-(1997), glutamic- (2004), and asparagine-peptidase (2010).
aspartate protease (e.g.HIV-1 protease)	Active site using twin Aspartate; relate to Human HIV disease	
Bc1 complex		During Quinol oxidation
human serum albumin		Type: ESPT
Cytochrome P450 cam	Catalyze the redox the organic molecules	Type: PCET
Oxidase		
Glucose oxidase		Type: PCET
Quinoprotein amine oxidase (Quinoprotein)	Metabolism of Nitrogen	Direction: Event happened per cycle: Type:
Reductase		
Nitric oxide reductase	Fix of nitrogen	Type: PCET
Fumarate reductase		Type: LRPT
copper-dependent nitrite reductase		Type: LRPT
cyt cd1 Nitrite Reductase		Type: PCET
Class I Ribonucleotide Reductase	catalyzes the formation of deoxyribonucleotides from ribonucleotides	Type: PCET
Others		

Ni-Fe hydrogenase	Metabolism of molecular hydrogen; for some bacterial as energy source	Direction: Event happened per cycle: 3? Type:
DNA photolyse	catalyzes the DNA repair	His→6-4PP Type: PCET
Carbonic anhydrase/ Human carbonic anhydrase II	Catalysis of hydration of carbon dioxide to produce bicarbonate.(one of the fastest enzyme)	Direction: Zn bind H ₂ O→solvent Event happened per cycle: Type:LRPT
Soybean lipoxygenase		Type: PCET
Superoxide Dismutase		Type: PCET
4-Oxalocrotonate Tautomerase		Type: PCET
Gramicidin A	Form an ion channel	Type: LRPT
Influenza Virus M2 Protein	Form an ion channel to dissolve the envelop of the virus and insert into the target cell membrane	Type: PCET

Jan22: 31 proteins listed

VITA

SHUO DAI

Candidate for the Degree of

Master of Science

Thesis: FIRST PRINCIPLE COMPUTATIONAL STUDIES ON HYDROGEN BOND
SWITCH IN BIOLOGICAL PROTON TRANSFER

Major Field: Physics

Biographical:

Education:

Completed the requirements for the Master of Science in your major at
Oklahoma State University, Stillwater, Oklahoma in July, 2013.

Completed the requirements for the Bachelor of Science in your major
at Nanjing University, Nanjing, China in 2004.

Experience:

Professional Memberships: